MODELING OF BRITTLE AND DUCTILE MATERIAL DRILLING USING SMOOTHED-PARTICLE HYDRODYNAMICS

A Thesis

by

MAHSA TAJDARI

Submitted to the Office of Graduate and Professional Studies of
Texas A&M University
in partial fulfillment of the requirements for the degree of

MASTER OF SCIENCE

Chair of Committee,	Bruce Tai
Co-Chair of Committee,	Arun Srinivasa
Committee Member,	Mathew Kuttolamadom
Head of Department,	Andreas A. Polycarpou

May 2016

Major Subject: Mechanical Engineering

ABSTRACT

The objective of this study is to investigate smoothed particle hydrodynamics (SPH) method in simulating drilling process of both brittle and ductile materials. Drilling simulation is commonly performed by finite element method (FEM); however, it is challenging when applied to small debris generated by brittle materials or special cutting tools, due to the inability to capture small chip interactions. SPH was originally developed for flow analysis but has been recently used in cutting research. In this study, SPH is compared with FEM by four case studies. The results show that SPH can simulate ductile drilling, but the chip formation and forces are not as reasonable as FEM. On the other hand, SPH can capture small fragmented debris in brittle material drilling, which cannot be done by FEM with an equivalent mesh size. SPH method is also found to be affected by the distance between the particles (element size in FEM) and numerical errors on the free surfaces, both of which require further investigation beyond this paper.

ACKNOWLEDGMENTS

I would like to thank my committee chair, Dr. Bruce Tai, and my committee members, Dr. Kuttolamadom and Dr. Srinivasa for their guidance and support throughout the course of this research.

Thanks also go to my friends and the department faculty and staff for making my time at Texas A&M University a great experience. I also want to extend my gratitude to the Department of Mechanical Engineering for the financial support.

Finally, thanks to my mother, father and my younger sister for their encouragement and love.

TABLE OF CONTENTS

Page

LIST OF FIGURES

Page

LIST OF TABLES

Page

CHAPTER I

INTRODUCTION

1.1 Drilling

Drilling is a common machining process and has applications in different fields including geoscience for drilling rocks[1], biomechanics for drilling bone tissue [2] and in the industry for drilling metals [3]. Based on the application, the work-material could be brittle, ductile, or a combination of both [4]. A better understanding in drilling mechanism and chip formation of different materials can help design the tool, ensure the hole quality, and avoid damaging the tool and workpiece.

Numerous studies have been presented in the past decades to analyze drilling in both ductile and brittle materials using analytical and experimental methods. For example, Williams [5] developed a chip formation model and an indentation model to simulate drilling in metals. The equations were derived to predict the total torque and thrust force for a given cutting condition, drill geometry, and the work material. Yuan et al. [6] adopted the brittle fracture mechanics to model the cutting force for carbon-fiber reinforced plastics. Ke et al. [7] analyzed the forces and continuous chip formation process with two models to predict spiral and string chip formation. However, these analytical and empirical models were specifically tuned for certain conditions. Chip formation, chip interaction with tools, and its morphology as a function of material properties have rarely been discussed.

1.2 Finite element modeling of cutting mechanics

To advance the simulation flexibility for a wide variety of drilling scenarios and three-dimensional visualization of chip formation, the numerical method, Finite Element Method (FEM), has opened a new paradigm. FEM has been used in simulating machining processes of various materials such as metals [3], composites [4], and biological tissues [8]. FEM has also been widely used to study the chip formation of orthogonal cutting for ductile materials [9-11]. However, despite the capabilities of FEM, the accuracy and correctness of simulation results significantly rely on the model setups, such as mesh size, arrangement, element type, and element damage model. Additionally, FEM suffers from the drawback of leading large mesh distortion which is an evitable part of drilling simulation. This issue implies the use of arbitrary Lagrangian-Eulerian (ALE) method and remeshing techniques which are known to be time consuming and to loss of stresses during remeshing. Unfortunately, the inability of FEM in problems involving moving boundaries and free surfaces is often the trade-offs with the computational time [12, 13].

Of particular challenge is that when an element experiences damage, it is removed from the model to mimic material failure [14]. Therefore, if a drilling process simulation involves element removal but does not have adequately fine mesh to form a chip, the chip can become fragmented, and the drilling force will be discontinuous. To balance between the mesh size and computational time, commercial software, such as Third Wave Systems [15], uses adaptive meshing method at each time increment to refine the cutting zone mesh and thus minimize the unrealistic chip formation and force generation. However, fine mesh is not an absolute solution for all materials; exceptions are composites and brittle

ceramics. For example, Usui et al. [16] needed to employ cohesive elements to simulate drilling of carbon-epoxy composites that contains elimination and chip fragments. Che et al. [17] used FEM to simulate orthogonal cutting of rock, but the forces were underestimated likely due to the loss of elements and their interactions with the cutting tool, despite the use of extremely fine mesh. Therefore, the objective of this project is to study an alternative numerical model, Smoothed Particle Hydrodynamics (SPH), for drilling process simulation, particularly in brittle materials.

1.3 Smoothed particle hydrodynamics method in cutting mechanics

The proposed SPH is a mesh-free method that was first employed for astrophysics application in 1977 and has gradually been utilized in continuum mechanics scale [18]. SPH has been widely used to obtain an approximate solution for the equation of fluid dynamics by replacing the fluid with a set of particles [19]. This is a method that links the continuum mechanics and fragmentation in a natural way. Different from FEM, SPH does not require a gridded domain to solve problems. Thus, it can handle problems involving free surfaces, deformable boundaries, moving interfaces, extremely large deformation and crack propagation [5]. Besides classical hydrodynamics, SPH may be applied to many areas of mechanics. Therefore the term “hydrodynamics” may be intrepretted as mechanics in general. However, the main application of SPH is in lagrangian continum mechanics. The earliest application of SPH is in fluid dynamics [18]. This method has been gradually extended to simulate the fracture of brittle solids[20], metal forming[21], high velocity impact[22], explosion [23] and metal cutting [18]. Villumen et al. and Limido et al. [18, 24] simulated the orthogonal cutting defining Johnson-cook (J-C) model

for aluminum to obtain the cutting forces and to simulate chip formation. Metal cutting involves all the process including milling turning and drilling[25]. Drilling is the most widely used machining process that not only has application in automobile industry and aerospace industry [14] but also has applications in house care, orthopedic surgery[2] and large scale drilling including rock drilling and soil drilling[1].

1.4 Objective and research method

The objective of this research is to study the feasibility of using SPH for material removal process for both ductile and brittle material. Drilling is a complex machining process [14]. Orthogonal cutting is usually employed to investigate the interaction between the tool and cutting edges. This method is a 2D material removal process. Therefore, in this research orthogonal cutting is utilized to study the cutting force and chip formation in SPH and FEM. Aluminum is selected to represent the ductile materials, which is commonly simulated by FEM. Cortical bone is used as the brittle material since there is currently no suitable numerical model for bone drilling. Since Finite element has been widely used to simulate the metal cutting process, this method adopted as the baseline of this research. That is, SPH is compared with FEM by creating identical SPH and FEM case studies generated by ABAQUS/EXPLICIT. The expected outcome of this study is to understand the capability of SPH in cutting simulation and investigate the limitations. Chapter II explains the modeling setup of orthogonal cutting and material selection. Chapter III discusses the effect of damage criteria in SPH and FEM. In chapter IV, cutting force and chip formation of FEM and SPH models are compared with different number of particles (SPH) and elements (FEM). By utilizing the points obtained from

chapter III and IV, a 3D cutting model for ductile and brittle material is developed in chapter V. Finally, chapter VI reviews the conclusion remarks of previous chapters. Fig. 1 demonstrates the research method of this research.

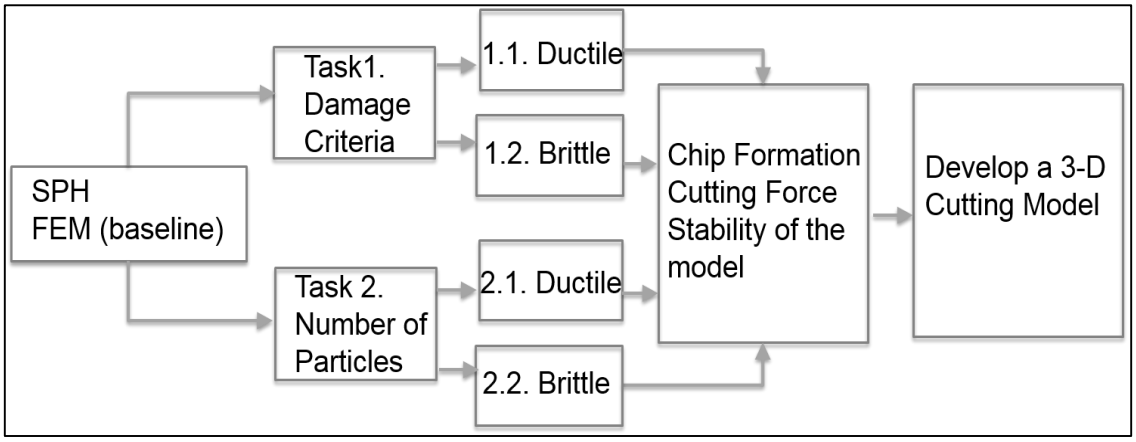

Figure 1: Research method

CHAPTER II

MATERIALS AND MODEL SETUP

This chapter describes the configuration model of orthogonal cutting and constructing of SPH model from FEM is explained. Material properties of ductile and brittle material is also explained.

2.1 Constructing SPH model

The SPH model was created based on the FEM model by converting the existing elemental nodes to SPH element PC3D, as the procedure is shown in Fig. 2. Note that SPH element is a point (or called particle) without an actual volume. The distance between two particles is known as the feature length, denoted by *l*, which serves as the smooth length used in the SPH Kernel function to describe the continuum of the-particle-formed body. The feature length in SPH is equivalent to the FEM mesh size.

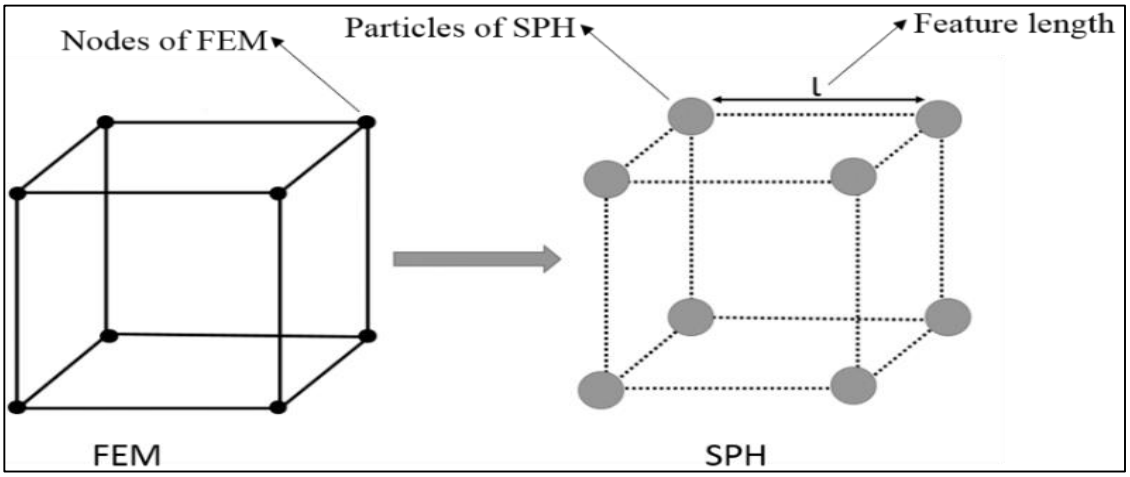

Figure 2: Transformation of one element of the finite element model into particles of the SPH model

2.2 Configuration of orthogonal cutting

In this study, the ABAQUS/EXPLICIT software was utilized to simulate the FEM and SPH models with an identical geometry for comparison. First, the workpiece mesh was generated using cubic C3D8R elements with an equal size as shown in Fig. 3(a). The dimensions of the whole workpiece were 5.0 mm × 10.0 mm × 2.0 mm. The top section of the workpiece (the uncut chip) is converted to SPH particles in SPH model as shown in Fig. 3(b).

It is possible to convert the entire FEM model to SPH model. However, to ensure the uncut region to have the same stiffness to support the cutting zone, a hybrid model consisting of both SPH and FEM domains was generated for SPH drilling simulation, as shown in Fig. 2. Since the SPH particles were converted from the elements, the nodal positions remained the same, and thus the nodes on the interface between SPH and FEM were completely overlaid. The "tie" function in ABAQUS was used to constrain the particles and nodes in all degrees of freedom to present a continuous material. For the boundary conditions of the models, the bottom nodes of the workpiece were fixed in X, Y and Z axes (BC#1), as described in Fig. 3.

The cutting tool is rigid with a clearance angle of 5 degrees and rake angle of 15 degrees. For the comparison purpose, the friction coefficient between the cutting tool and workpiece is 0.2. A reference point is defined on the cutter and the velocity of 400 mm/s is applied to this point on the negative X direction.

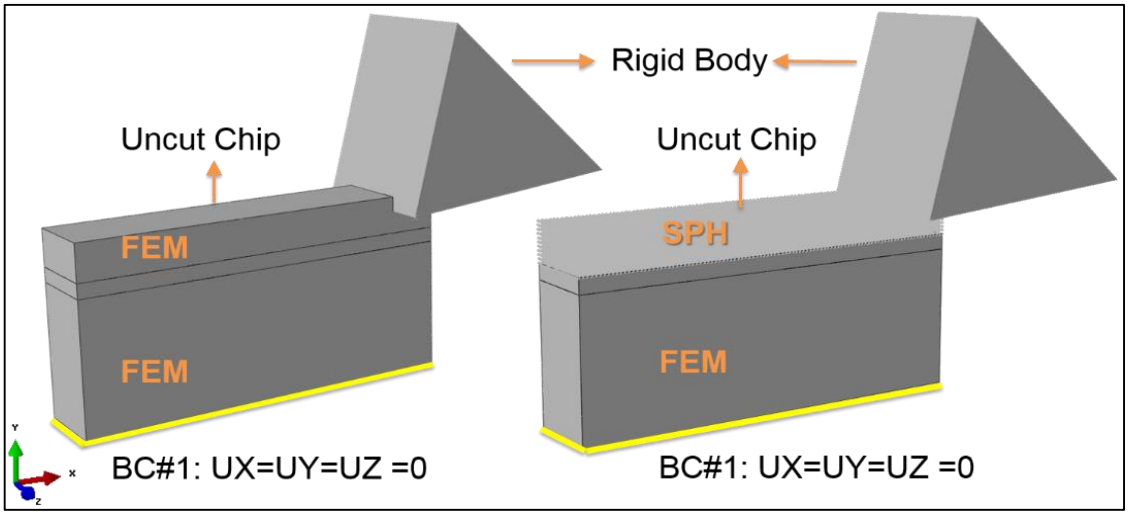

(a) FEM (b) SPH

Figure 3: Configuration of orthogonal cutting

2.3 Material selection

2.3.1 Ductile material

The ductile material was chosen to be aluminum 2024-T351, as the properties defined in Table 1. Aluminum is commonly used in manufacturing and aluminum drilling has been studied extensively. Johnson-Cook (J-C) material model is often used to represent the behaviors of aluminum. This model provides a comprehensive description of a metal's behaviors undertaking large strains, high strain rates, and temperature dependent visco-plasticity which happen in cutting processes. The J-C plastic model is presented by the following equation of the equivalent plastic flow stress (Eq. 1). The J-C parameters used to simulate Al2024-T351 workpiece are specified in Table 2 [26]. Effects of temperature and strain rate were not considered in this study.

$$\bar{\sigma} = \left(A + B\bar{\varepsilon}^{n}\right)\left[1 + C\ln\left(\frac{\dot{\bar{\varepsilon}}}{\dot{\bar{\varepsilon}}_0}\right)\right]\left[1 - \left(\frac{T - T_{room}}{T_{melt} - T_{room}}\right)^{m}\right] \quad (1)$$

The J-C shear failure model was used as a damage initiation criterion (Eq. 2). The parameter values of Al2024-T351 are given in Table 2 [26]. The damage evolution was assumed based on the maximum displacement defined at 5 μm.

$$\dot{\bar{\varepsilon}}_{0i} = \left[D_1 + D_2 \exp(\mathrm{D}_3 \frac{P}{\bar{\sigma}}) \right] \left[1 + D_4 \ln(\frac{\dot{\bar{\varepsilon}}}{\dot{\bar{\varepsilon}}_0}) \right] \left[1 - D_5 \left(\frac{T - T_{room}}{T_{melt} - T_{room}} \right) \right] \qquad (2)$$

Table. 1. Mechanical properties of Al2024-T351

Density (kg/m3)	Elastic Modulus (MPa)	Poisson's ration
2700	73000	0.33

Table. 2. J-C Plastic and failure parameters for A2024-T351

A (MPa)	B (MPa)	N	D1	D2	D3	D4	D5
352	440	0.42	0.13	0.13	-1.5	0.011	0

2.3.2 Brittle material

The brittle material was chosen to be the cortical bone. Bone is relatively brittle since it typically has an infinitesimal plastic deformation in the tensile stress-strain curve [27]. Bone is also a common biological material dealt by surgeons every day. A brittle damage model was used to represent the cortical bone. The mechanical properties are shown in Table 3 [27]. A small plastic region was applied between the strain 0.0185 and 0.0330. Once the damage initiated, the damage evolution was set based the displacement of 1 μm. This would produce a fairly brittle behavior upon fracture.

Table. 3. Mechanical properties of bone

Density (kg/m^3)	Elastic Modulus (MPa)	Poisson's ration	Yield Stress (MPa)
2000	5396.7	0.3	100

CHAPTER III

EFFECTS OF DAMAGE CRITERIA DEFINITION

This chapter studies the effects of damage criteria on SPH for ductile and brittle material. Three case studies of SPH are developed, and the cutting force and chip formation of each case are compared with FEM results.

3.1 Damage criteria

To define damage in FEM, damage initiation and damage evolution are the two critical parameters to be defined. Damage initiation parameter provides material properties that initiate damage while damage evolution parameter determines the evolution of damage leading to eventual failure. These two points are illustrated in Fig. 4. In finite element model, if the damage initiation is not defined, the stress will continue increasing without element failure. On the other hand, SPH behaves differently. If the damage is not defined in SPH model, the material will naturally fail at a certain point due to particle distance (Fig. 4).

In regard to SPH, the literature survey shows two parties regarding the damage criterion definition. One group believes that damage parameters are not required to identify in SPH analysis since the element separation happens due to the loss of cohesion between neighboring particles [28, 29]. The other group, Limido et al. and M. Heinstein et al.[18, 30], believes that damage parameters are required to set to force the particle to separate at the defined failure criteria.

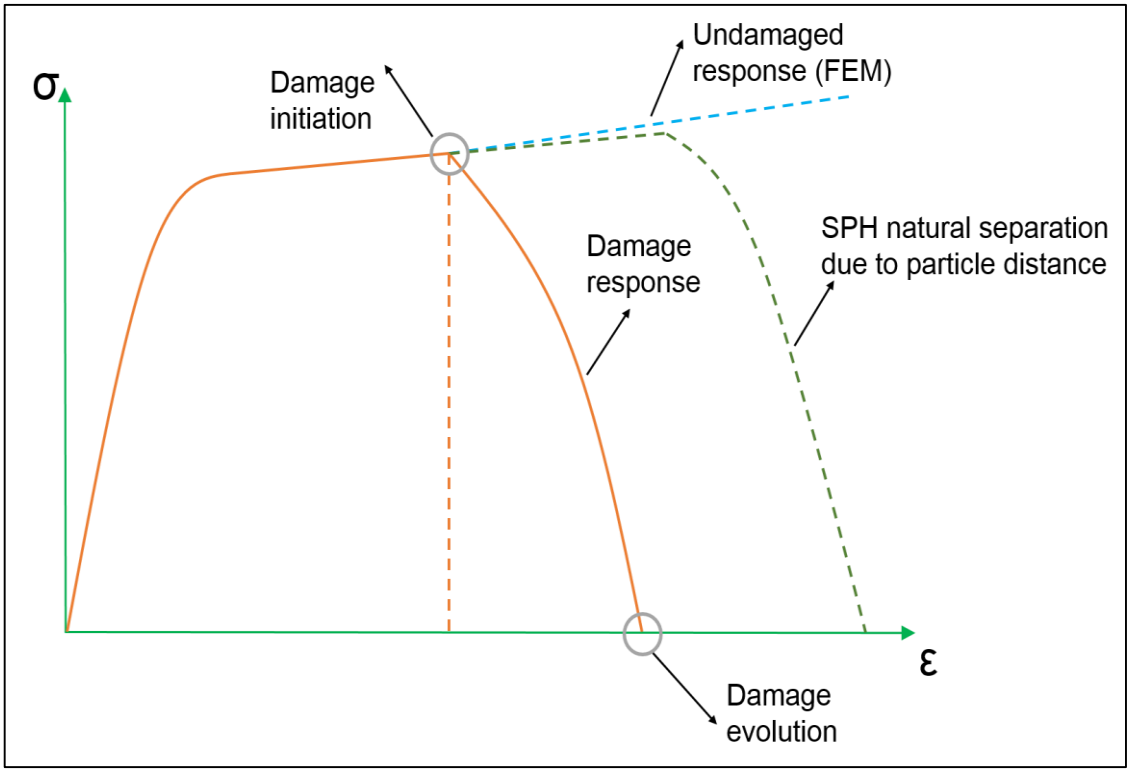

Figure 4: Configuration of damage criteria in FEM and SPH

3.2 Study method

To study the effect of damage criteria in SPH, three case studies are developed. In Case I, damage is defined; that is, the material separation occurs based on the natural separation of SPH. The Case II consists of damage initiation without defining damage evolution. In the next step, Case III, damage evolution is defined along with damage initiation. The cutting force and chip formation of three cases of SPH is compared with an identical finite element model. In the finite element model, damage criteria including damage initiation and damage evolution are defined in material properties. For each case study, the cutting force of the reference point located on the cutter is extracted.

3.3 Results

3.3.1 Ductile material

3.3.1.1 FEM

Aluminum is adopted as ductile material, and finite element model of orthogonal cutting is chosen as the baseline. The element size of FEM is 0.05 mm (the finest mesh size for the FEM) in the chip zone. Damage parameters including damage initiation and damage evolution are also defined. In FEM analysis, once an element reaches its damaged point, it is deleted from the model. In orthogonal cutting while the cutter moves toward the workpiece the elements are being separated and removed from the model due to the defined damage parameters (Fig. 5). The cutting force is oscillating due to element deletion but the average remains constant (Fig. 6).

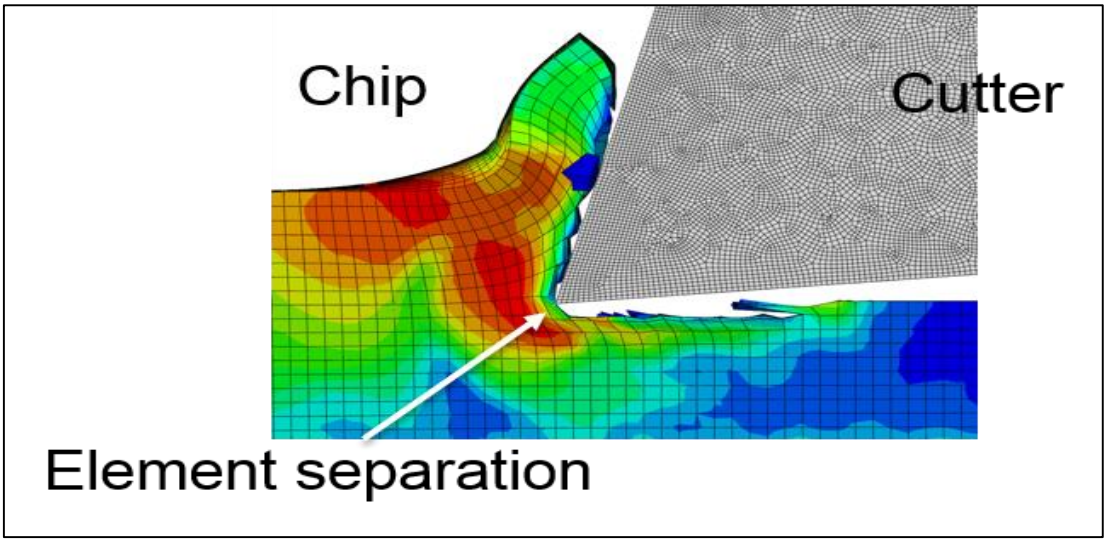

Figure 5: Material removal process in orthogonal cutting

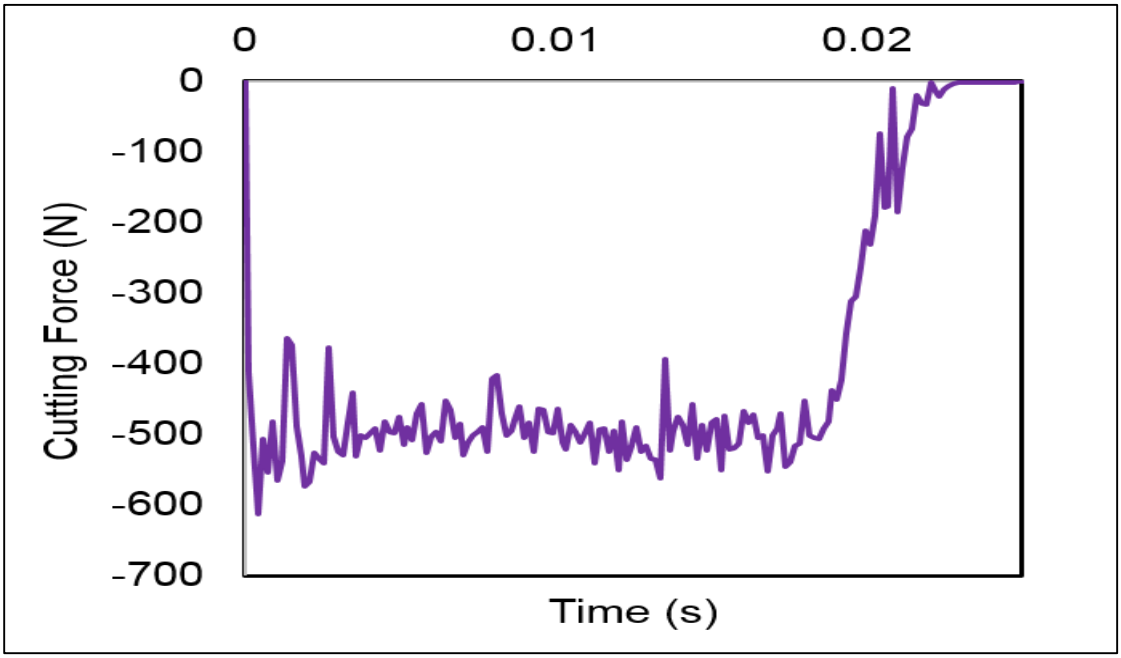

Figure 6: FEM result of orthogonal cutting for ductile material (cutting force)

The chip formation obtained from finite element analysis is shown in Fig. 7. Since the workpiece material is ductile, the chip is continuous.

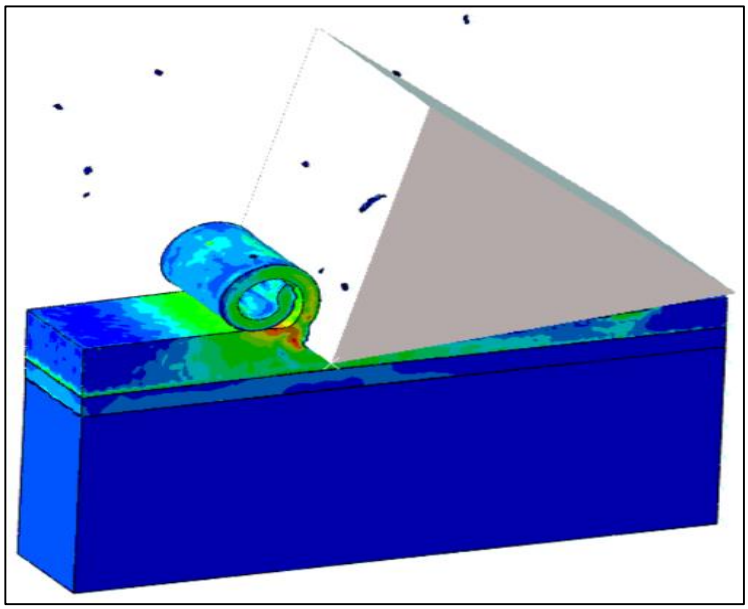
Figure 7: FEM simulation of orthogonal cutting

3.3.1.2 SPH

The results of the cutting force of Case I and Case II of SPH comparing to FEM result are extracted in Fig. 8. The chip formation mechanism of these two cases is investigated (Fig. 9). The results indicate that the cutting force and chip formation of these two cases are exactly identical.

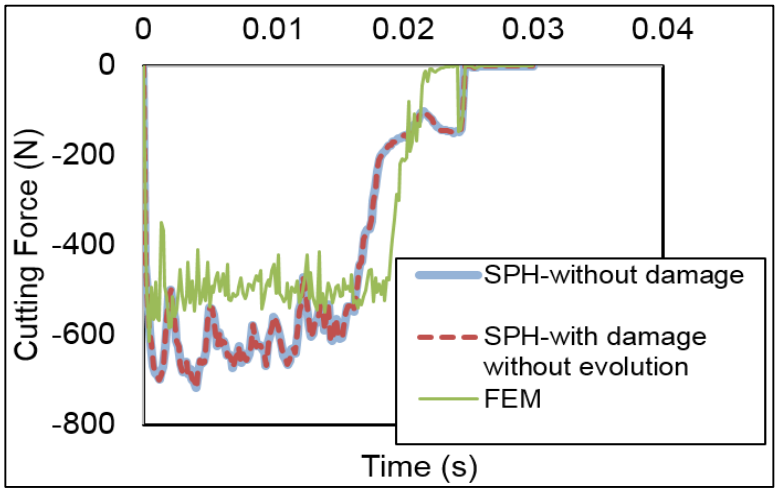

Figure 8: SPH result of Case I and Case II comparing to FEM results for ductile material.

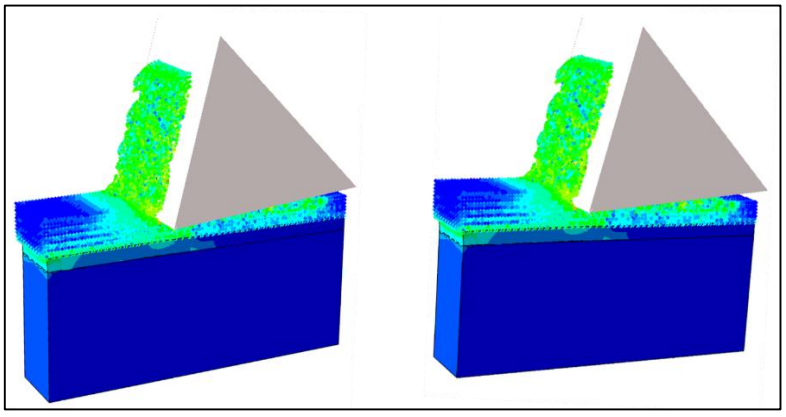

(a) Case I (b) Case II

Figure 9: Simulation result of SPH for ductile material (chip formation)

In the next step, damage evolution is considered to compare with Cases I and II. The results compared to FEM are shown in Fig. 10. By defining damage evolution, the model is being unstable and explode at a certain point. That is the reason why the time scale of Fig. 10 is 0.004 s, which is the step time of the first frame. At the end of the first frame, Case III (the model having all damage parameters including damage initiation and damage evolution) is exploded (Fig. 11).

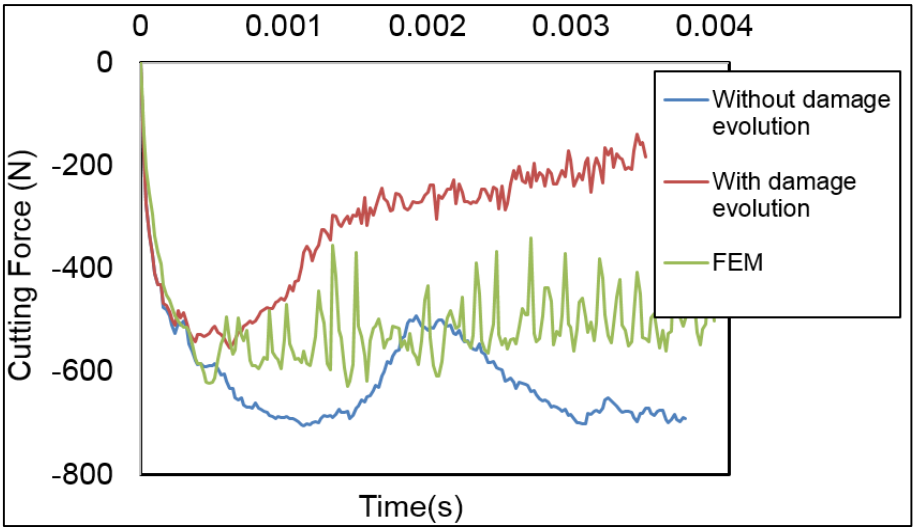

Figure 10: SPH result of Case II and Case III comparing to FEM result for ductile material

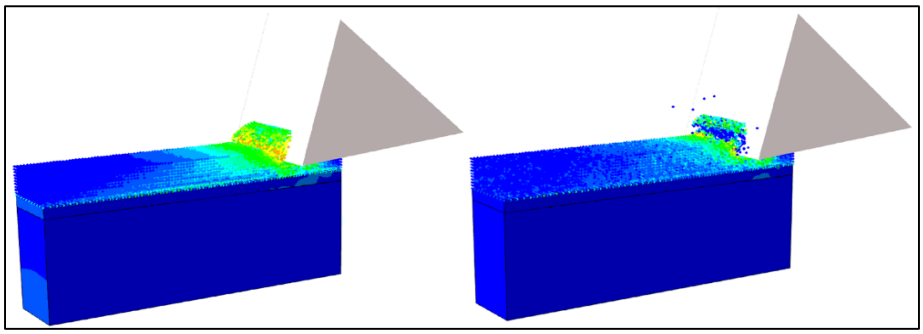

a) Case II b) Case III

Figure 11: Simulation result of SPH for ductile material

3.3.2 Brittle material

3.3.2.1 FEM

Similar to the previous case, FEM is used as the baseline to investigate cutting force and chip formation for brittle material. The workpiece material is cortical bone. Since the elements are removed from the model (Fig. 12), the cutting force is highly oscillated (Fig. 13). Because the material is brittle, fragmented chips are separate from the workpiece (Fig 14).

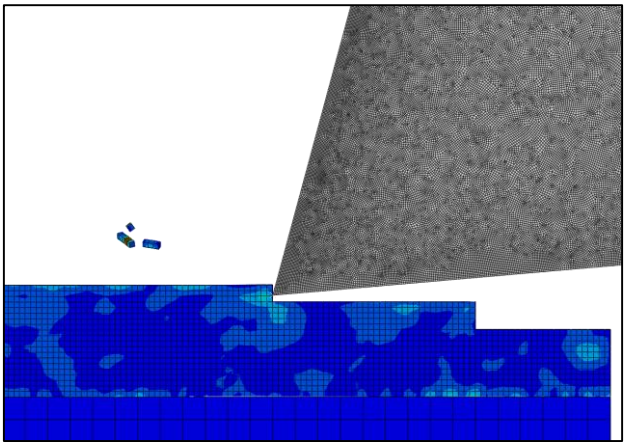

Figure 12: FEM simulation of material removal for brittle material

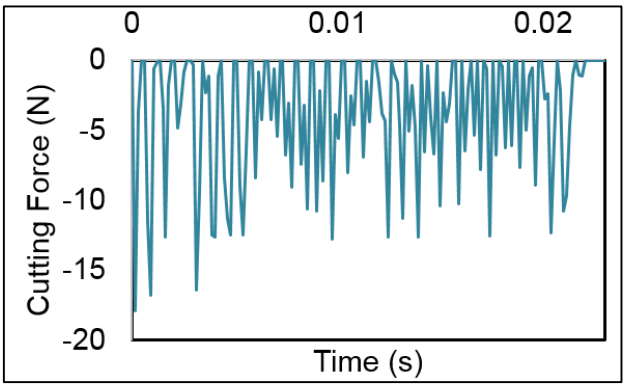

Figure 13: FEM result of brittle material

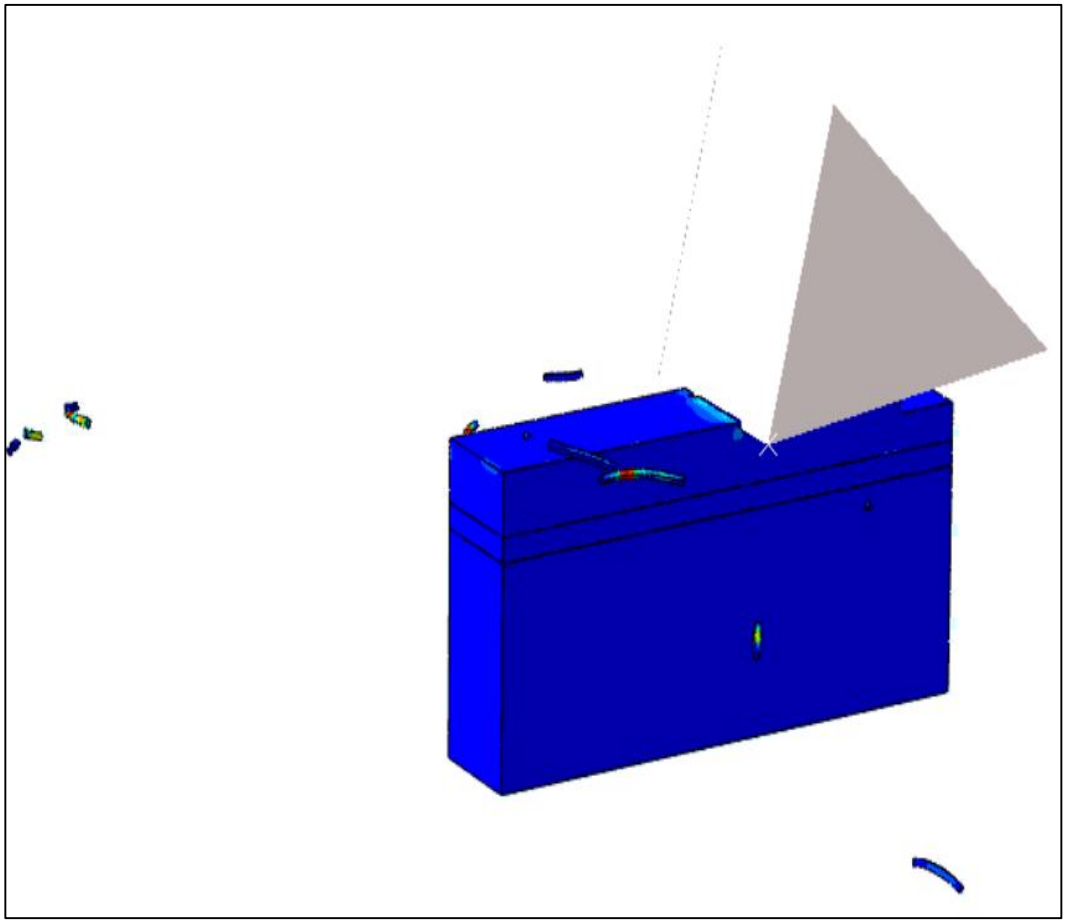

Figure 14: FEM simulation of orthogonal cutting of brittle material

3.3.2.2 SPH

The cutting force and chip formation extracted from Cases I and II shown in Figures 16 and 17. Similar to the previous case for ductile material these two cases are the same. The cutting force of Case III is significantly lower than those of Case I and Case II but is similar to the average of FEM results (Fig. 16). Since the material is brittle, it is expected to see broken chips; however, in Cases I and II the continuous chip is formed. In comparison, in Case III, when setting the damage initiation and damage evolution, the broken chips can be simulated as shown in Figure 17.

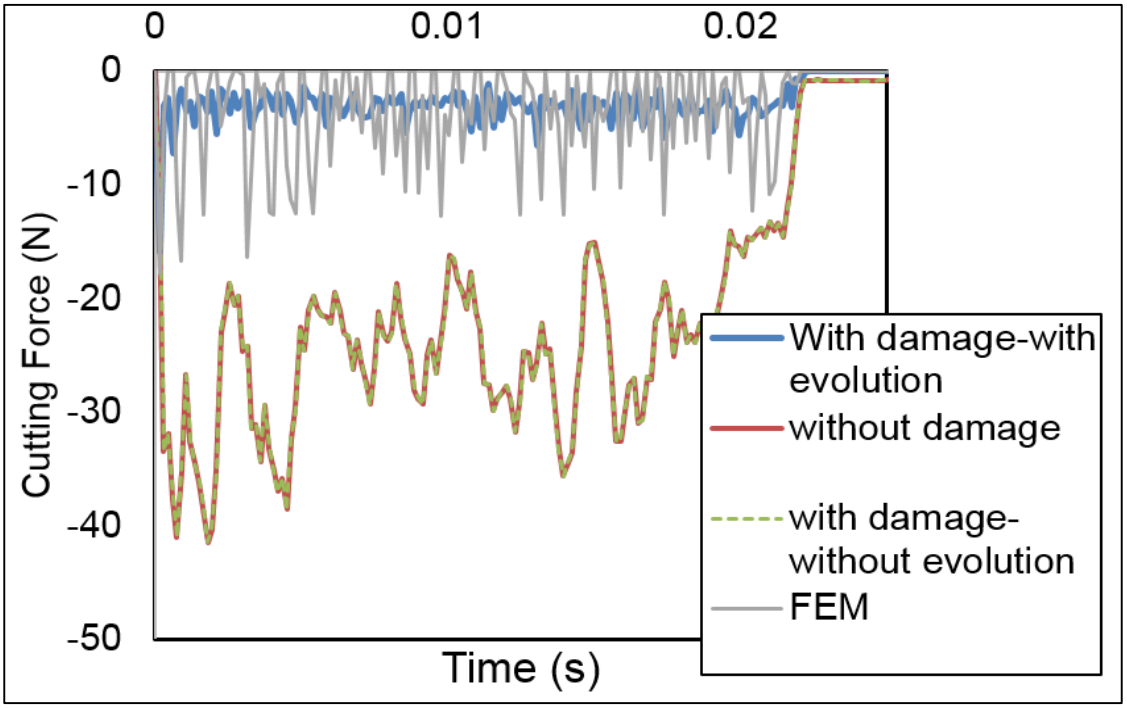

Figure 15: SPH result of cutting force comparing to FEM (brittle material)

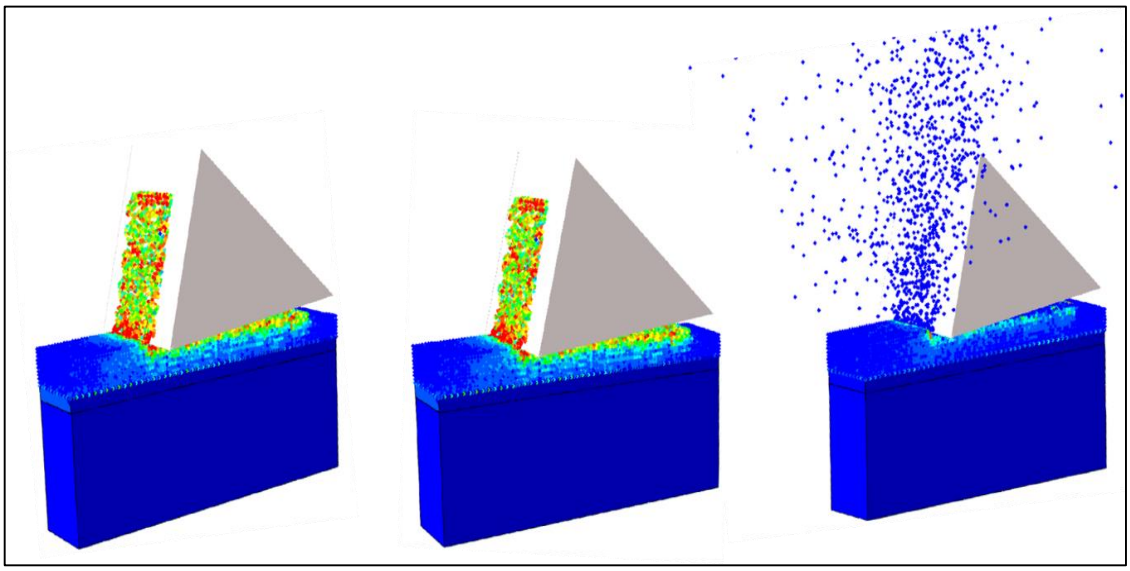

a) Case I b) Case II c) Case III

Figure 16: Simulation result of SPH with different damage criteria (brittle material)

3.4 Concluding remarks

3.4.1 Ductile material

In the preceding sections, the effect of damage parameters is investigated for SPH and FEM simulations. The results indicate that damage evolution must be defined along with damage initiation. However, if the work material is extremely ductile the material removal process may occur due to the natural separation of SPH, and there is no need to define damage parameters in this case. However, damage evolution may need for less ductile material to model broken chips.

Setting damage evolution in SPH analysis leads to the instability of the model. The remaining particles have larger momentum comparing to other particles that could lead to "explosion".

In conclusion, to simulate the material removal process for ductile material, damage property may not define to maintain the model stability. Also, SPH may not be used for chip formation since the chip looks stiffer compared to the identical FEM (will be explained in Chapter 3).

3.4.2 Brittle material

Damage evolution must be set to create fragmented debris and to obtain accurate force result, comparing three cases of damage parameters. If damage evolution is defined, SPH will show the broken chips while FEM cannot, due to the nature of element deletion. Also, the model stability is low because of the large momentum of the remaining particles that could lead to "explosion".

It is suggested to obtain accurate cutting force and chip formation; damage evolution is needed to be defined. Also, it is required to manually tune damage settings in ABAQUS subroutine to avoid explosion.

CHAPTER IV

EFFECTS OF PARTICLE DENSITY

This chapter focuses on the convergence study of particle density in SPH. Particle density is equivalent to the element size in FEM. To elaborate more, identical cutting conditions are designed with different particle distance (in SPH) and element size (in FEM) to investigate if the particle distance and number of elements will affect the result.

4.1 Model convergence

Convergence test is a numerical issue when dealing with finite element analysis [31]. The results of finite element analysis should be independent of number of particles. So, it is required to increase the number of particles to obtain converged results. SPH behaves in a similar way. So, to obtain trustable results from SPH analysis, it is needed to increase the number of particles to obtain converged results.

4.2 Method

To investigate the effect of number of particles the uncut chip is meshed with different number of particles. For ductile material the depth of cut is 0.4 mm and simulations are designed based on 2, 4 and 8 particles in uncut chip in SPH model which is identical to 2, 4 and 8 elements in finite element model. (Fig. 17).

In brittle material, the thickness of the uncut chip in 0.09 mm since the thicker depth of cut may lead to “explosion”. In another word, the bottom nodes of the workpiece are fixed and the material is brittle. Therefore, cutting larger thickness of the work material will break the entire workpiece. Two case studies are designed for brittle material. The

number of particles in the uncut chip of SPH is 1 and 2 which is equivalent to 1 and 2 elements in FEM (Fig. 18).

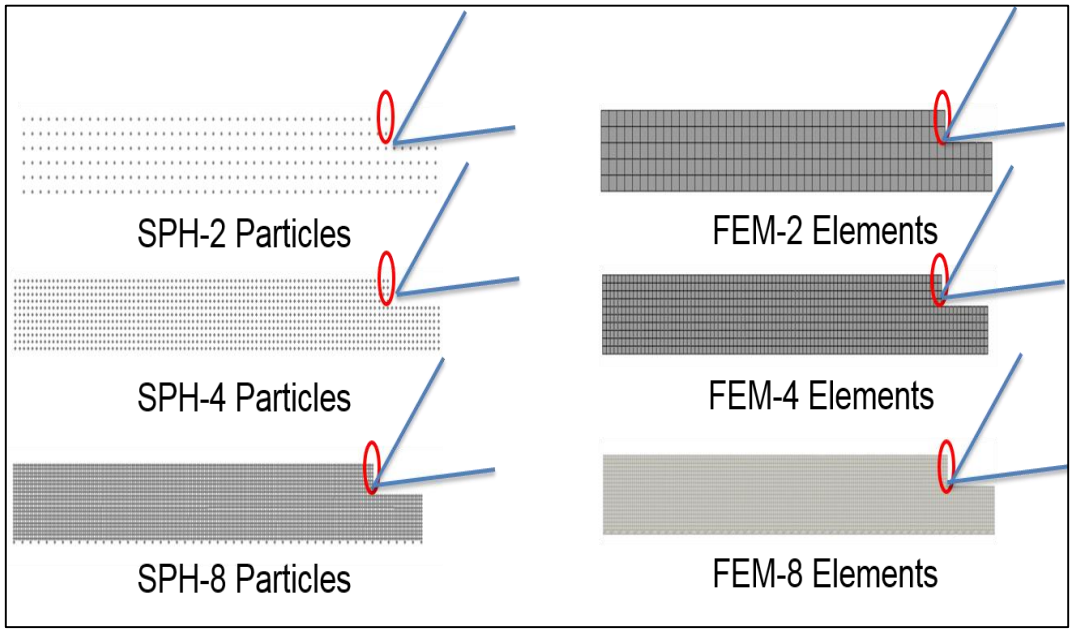

Figure 17: Different number of particles of SPH vs. different number of elements in FEM for ductile material

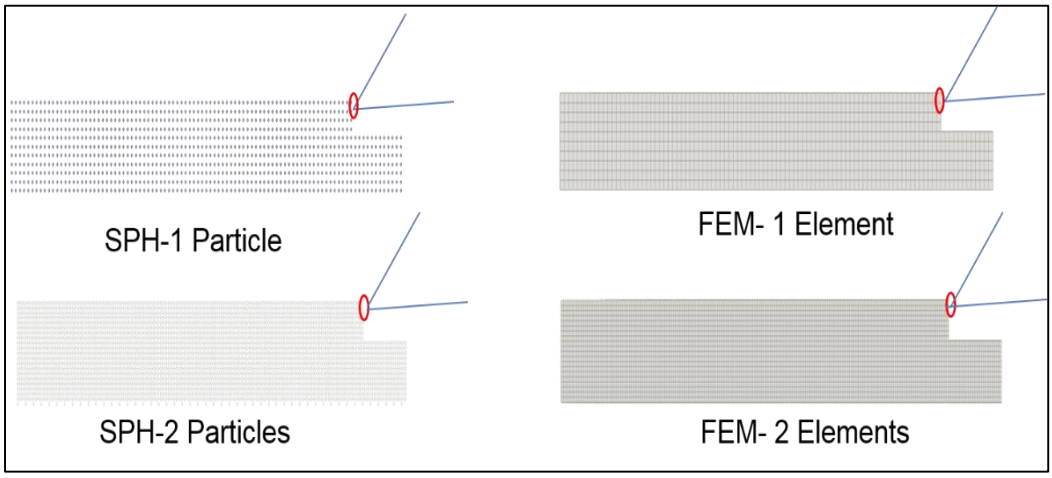

Figure 18: Different number of particles of SPH vs. different number of elements in FEM for brittle material

4.3 Results

4.3.1 Ductile material

4.3.1.1 FEM

Similar to previous chapter, aluminum is chosen for the workpiece material. Three case studies are set to with 2, 4 and 8 elements in the uncut chip. By increasing the number of particles, the deleted volume from the workpiece is becoming less. Therefore, the cutting force is high (Fig. 19) and smooth and chip is continuous (Fig. 20).

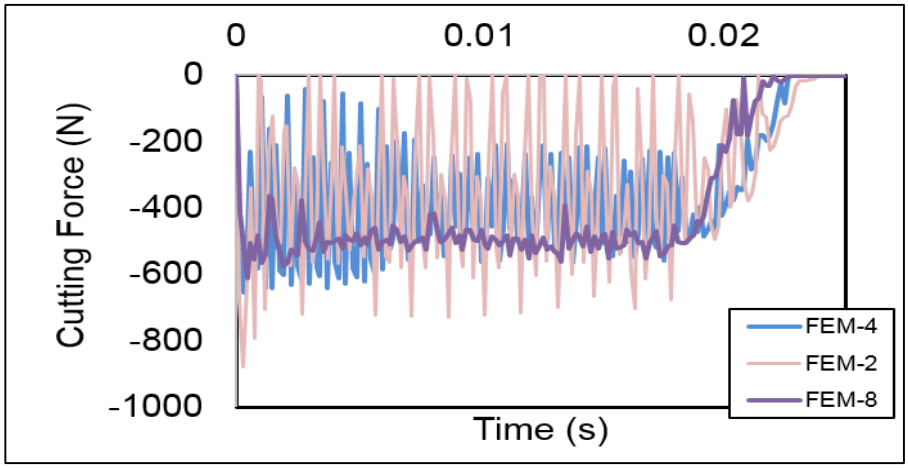

Figure 19: FEM result of cutting force for different number of elements (ductile material)

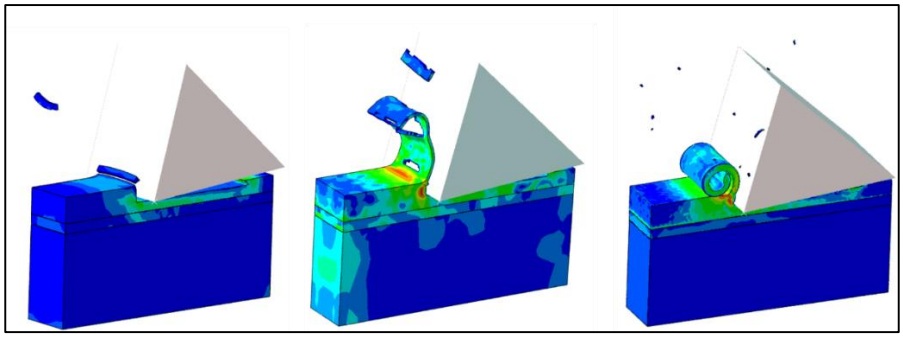

(a) Two elements (b) Four elements (c) Eight elements

Figure 20: Simulation result of FEM for different number of elements (ductile material)

4.3.1.2 SPH

Similar to the FEM, SPH models are created based on 2, 4 and 8 particles in the uncut chip zone. The chip formation is similar in three cases (Fig. 22) but the cutting forces behave differently. Setting 8 particles in the uncut chip will lead to less cutting force comparing to setting 2 and 4 particles (Fig. 21).

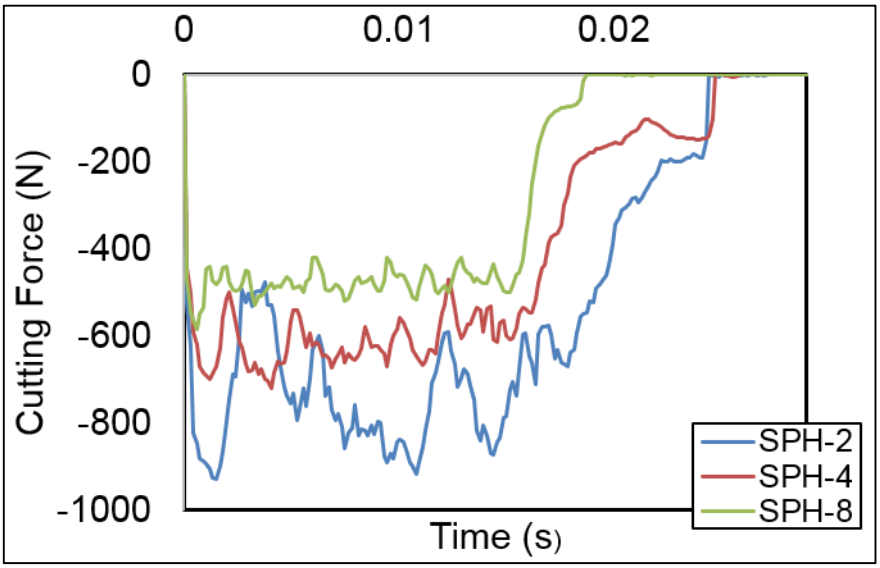

Figure 21: SPH results of cutting force for different number of elements (ductile material)

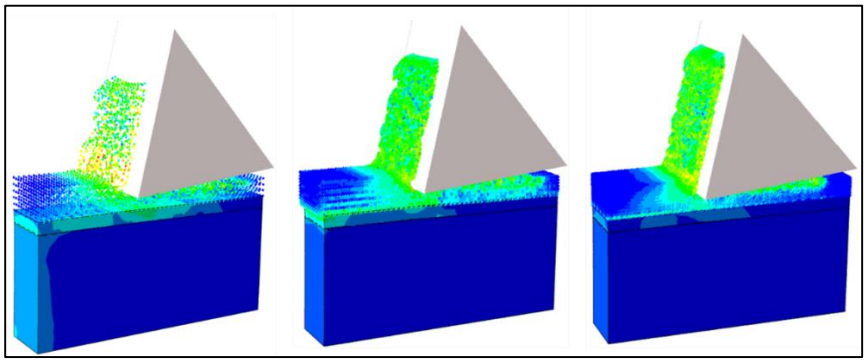

(a) Two particles (b) Four particles (c) Eight particles

Figure 22: Simulation results of SPH for different number of elements (ductile material)

4.3.2 Brittle material

4.3.2.1 FEM

Similar to other case studies for brittle material, bone is used for the workpiece material. Two case studies are utilized in the FEM of orthogonal cutting. Case one consists of one element in the uncut chip and case two has two elements. The cutting force is illustrated in figure 23. The chip is supposed to be fragmented due to the brittleness of the workpiece. Therefore, increasing the number of elements may lead to simulate broken chips more accurately since the less volume is removed from the model (Fig. 24) .

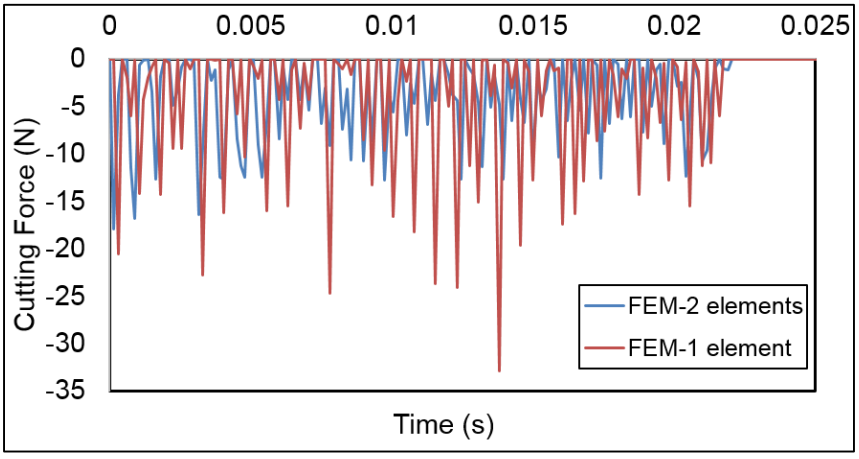

Figure 23: FEM result of cutting force for different number of elements (brittle material)

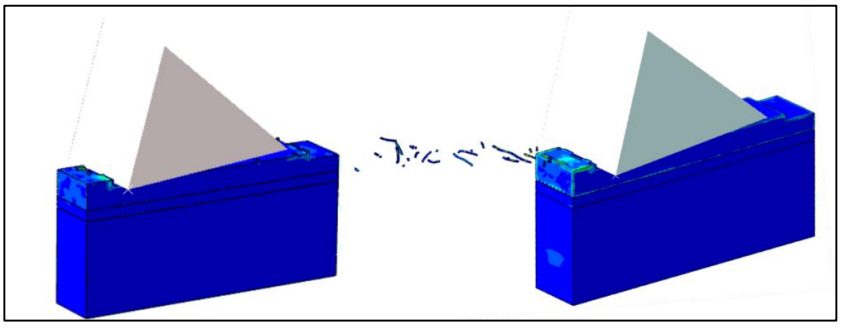
(a) One elements (b) Two elements

Figure 24: Simulation result of FEM for different number of elements (brittle material)

4.3.2.2 SPH

The identical condition of the FEM is applied to the SPH model for one and two particles in the uncut chip. The results of the cuttin force are shown is fig. 25. In case two (two particles) the simulation is not completed since the results are not converged likely due to the problem of damage setting. So, the results of the 2 particle case are shown for the first frame (fig. 26).

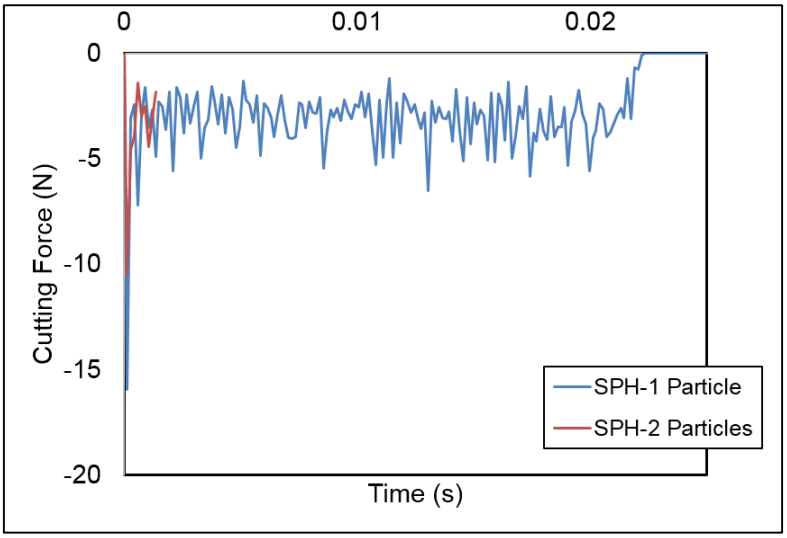

Figure 25: SPH result of cutting force for different number of elements (brittle material)

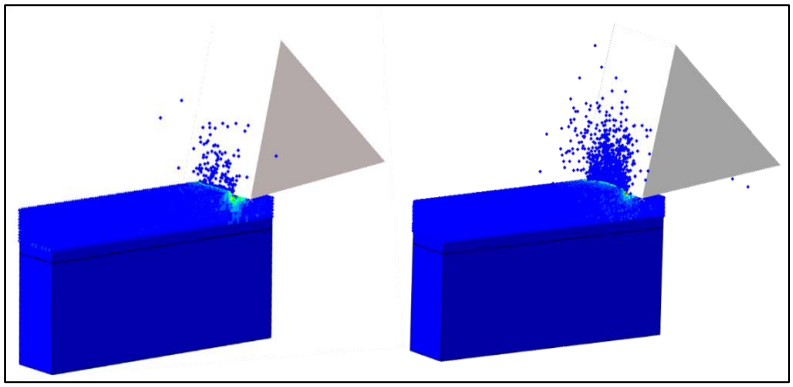

(a) One particle (b) Two particles

Figure 26: Simulation result of SPH for different number of elements (brittle material)

4.3.3 Comparison between FEM and SPH

4.3.3.1 Ductile material

Both FEM and SPH will give the result of 500N by using maximum mesh size. But the disparate point of these two methods is FEM converges from lower values to high one (Fig. 27) while SPH converges from higher to lower. In other words, the less number of particles in SPH will give a higher force. This fact can be clarified due to the discontinuity problems at the boundary of SPH which is clarified in the next section.

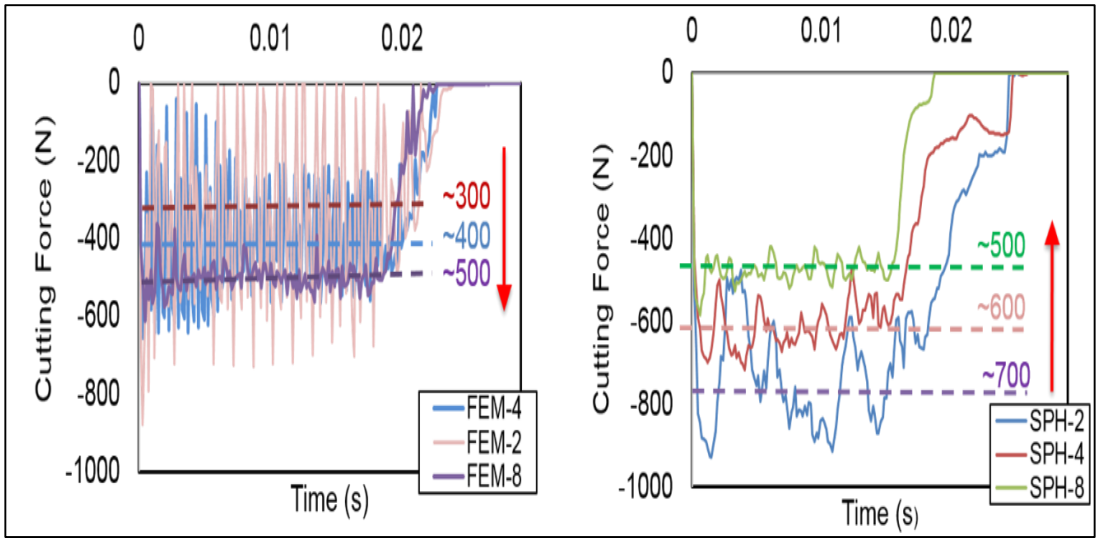

(a) FEM (b) SPH

Figure 27: Comparison between the results of FEM and SPH for ductile material

4.3.3.2 Brittle material

Due to element deletion nature of FEM the cutting force is oscillating while the result of more particles is smoother and the average is close to that of SPH model. Also, in the SPH model, fine particle arrangment makes the simulation difficult to converge (fig. 28).

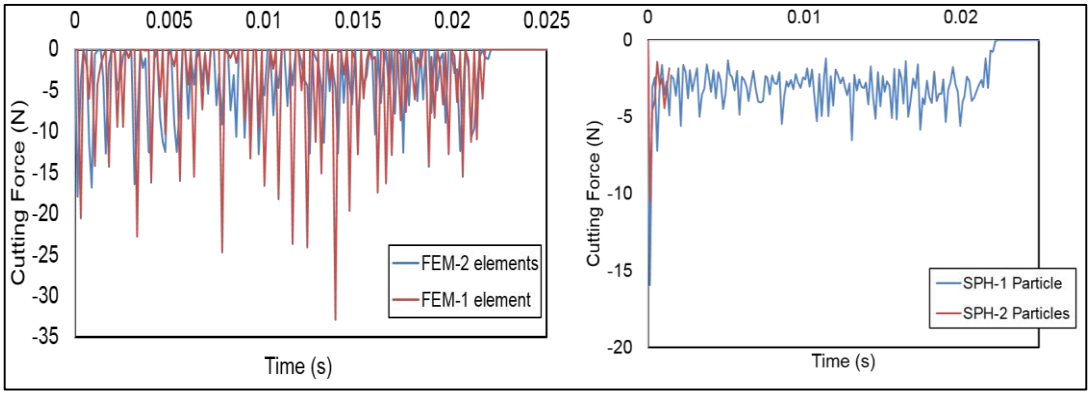

(a) FEM (b) SPH

Figure 28: Comparison between the results of FEM and SPH for brittle material

4.4 Truncated kernel function

Kernel function is discontinuous at the boundary of SPH. Therefore, the particles at the boundary demonstrate higher stress. As shown in figure 29 the inside particles have perfect kernel function while the boundary particles have truncated kernel function. To elaborate more, a simple four point bending is performed following a standard ASTM dimensions (6.5 mm × 13 mm × 156 mm) (fig. 30).

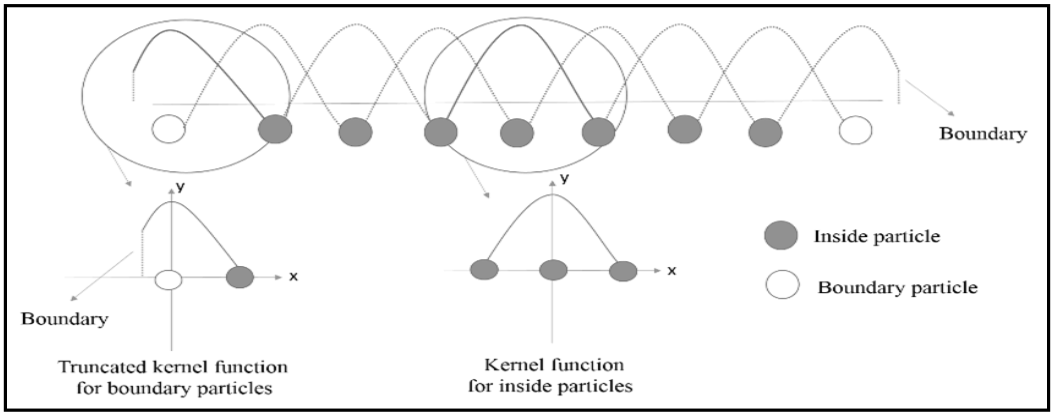

Figure 29: Configuration of kernel function on boundary particle and inside particles.

The bottom two pins are fixed in all directions (BC#1) and the two top pins have the velocity of 5 mm/s in negative Y direction (BC#2).

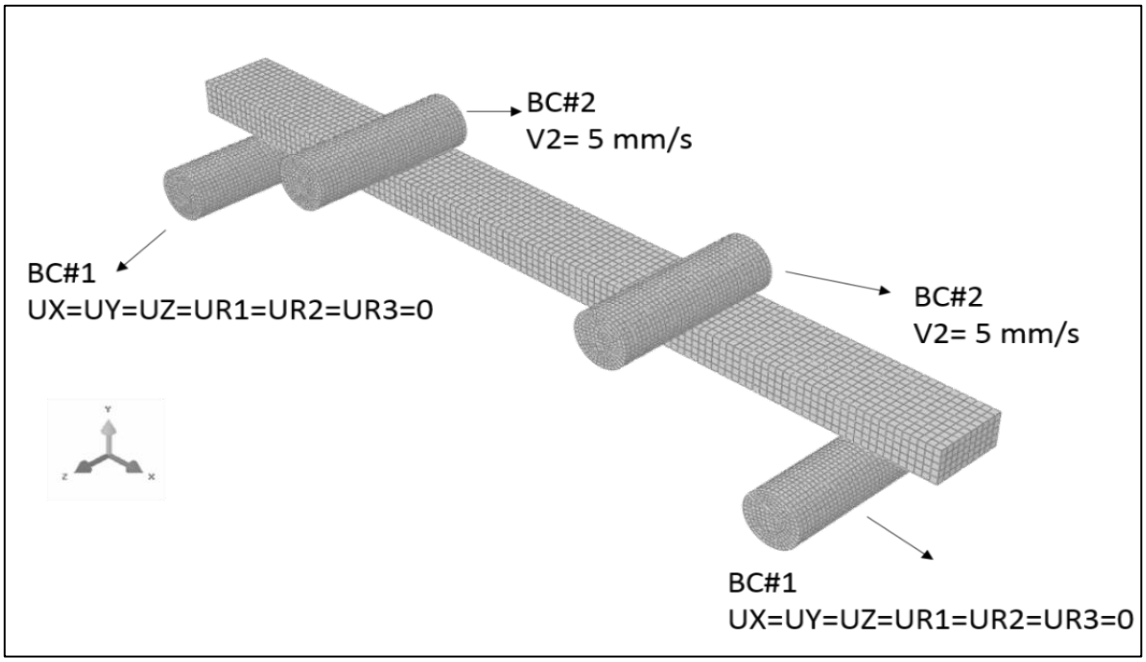

Figure 30: Configuration of four point bending

To avoid penetration the interaction is defined between the outer surfaces of every elements with the surfaces of the support pins. And finally, the part is meshed with cubic C3D8 elements.

The pins are defined as rigid body and the work material is set to be Al6060-T6. To compare the SPH with FEM the reaction force in Y direction is extracted from the reference point located on the top pins. SPH model is generated from finite element model. As it is shown in figure 31, the particles on the boundary of SPH has higher stress comparing to the inside particle. But this question may arise that why increasing the number of particles will lead to smaller cutting force in the orthogonal cutting model?

Figure 32 shows a simple math to elaborate this fact. First, the geometry meshes with a few number of particles and the ratio of boundary particles to the total number of particles is calculated. As shown in figure 32 by increasing the number of particles this ratio is becoming smaller. Therefore, the effect of the truncated kernel function of the boundary particles is alleviated, and the cutting force is less.

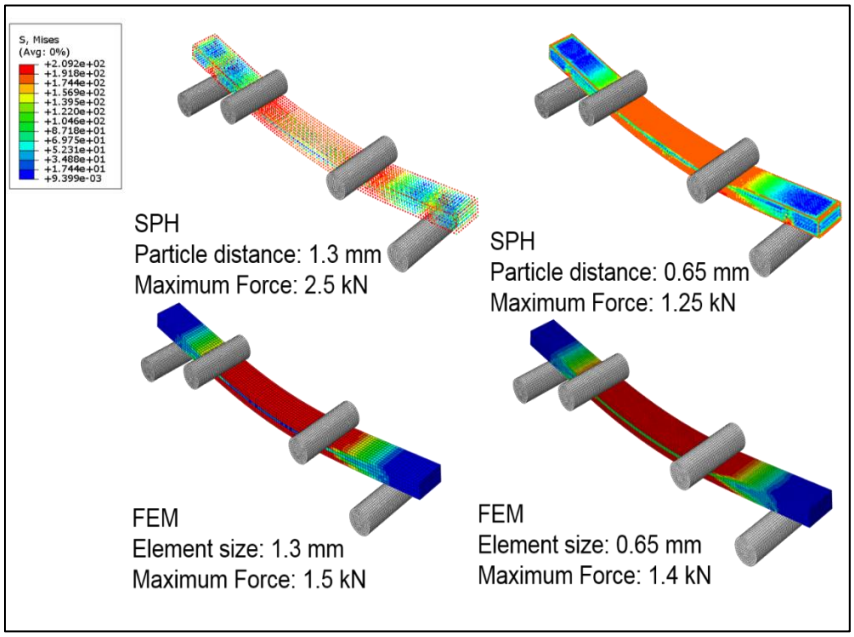

Figure 31: Comparison of boundary particles between FEM and SPH

4.5 Concluding remarks

This section investigates the effect of particles distance on SPH analysis which is equivalent to the effect of number of elements in FEM. The cutting force and chip formation is obtained for the ductile material. In SPH model, small particle distance may lead to obtain accurate results while larger particle distance demonstrates the reasonable behavior of material although overestimated.

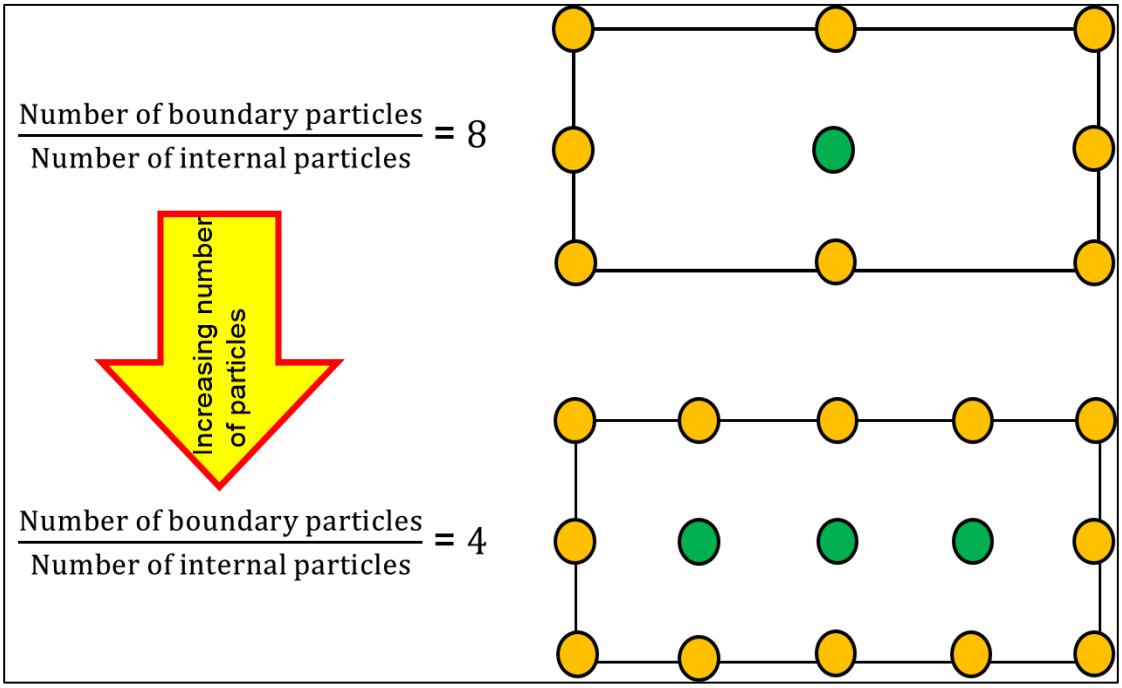

Figure 32: Increasing the number of particles to investigate the effect of boundary particles

CHAPTER V

SIMULATION OF 3-D CUTTING MODEL

In the previous chapters, the effect of the damage criteria and number of particles in FEM and SPH analysis is investigated for ductile and brittle material. So, the last part of the research would be how to incorporate the knowledge to create a 3D drilling simulation.

5.1 Model setup

5.1.1 Workpiece and mesh configuration

In this study, the ABAQUS/EXPLICIT FEM software was utilized to simulate the FEM and SPH models with an identical geometry for comparison. First, the workpiece mesh was generated using cubic C3D8R elements with an equal size (0.05 × 0.05 × 0.05 mm) as shown in Fig. 33(a). The dimensions of the whole workpiece were 3.0 mm × 3.0 mm × 1.1 mm. This model was made to simulate a full cutting edge-and-workpiece contact during drilling, so a cone shape with a point angle of 90˚ was created in the workpiece by removing geometrically correspondent elements, as shown in Fig. 33(b).

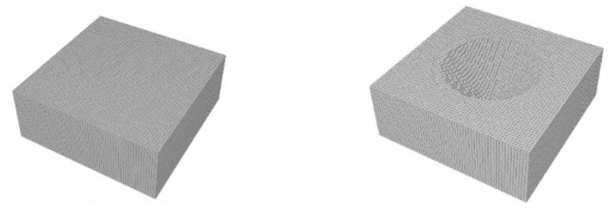

(a) (b)

Figure 33: (a) Initial finite element model and (b) modified finite element model with removed cone shaped elements

The SPH model is generated based on the FEM by converting the existing elemental nodes to SPH element, PC3D. The feature length (distance between the particles) was set to be 0.05 mm which is equivalent to the FEM mesh size.

It is possible to convert the entire FEM model to SPH model. However, to ensure the uncut region to have the same stiffness to support the cutting zone, a hybrid model consisting of both SPH and FEM domains was generated for SPH drilling simulation, as shown in Fig. 34. Since the SPH particles were converted from the elements, the nodal positions remained the same, and thus the nodes on the interface between SPH and FEM were completely overlaid. The "tie" function in ABAQUS was used to constrain the particles and nodes in all degrees of freedom to present a continuous material. For the boundary conditions of the models, the bottom four edges of the workpiece were fixed in X, Y and Z axes (BC#1), as described in Fig. 34.

5.1.2 Drilling tools and contact definition

Two drilling tools are selected in this study, regular twist drill and Kirschner wire (K-wire), since they have completely different drilling characteristics. Twist drill normally consists of two flutes to remove and evacuate the work-material. K-wire, in contrast, has a trocar tip with three facets. Thus, the rake angle of each cutting edge is highly negative, which produces fragmented chips. Both tools were made to have an identical point angle of 90° and a diameter of 2 mm to match with the model's cone shape, as shown in Fig. 35. They were created as a rigid body shell in both FEM and SPH.

K-wire in bone drilling is of particular interest since it is commonly used in orthopedic surgery. Due to the lack of positive rake angles in cutting and the brittle nature

of bone, K-wire drilling often creates dusty debris. The accumulated debris at the K-wire tip creates a tremendous amount of heat [32]. Being able to analyze bone cutting and chip formation will be beneficial in surgical tool design.

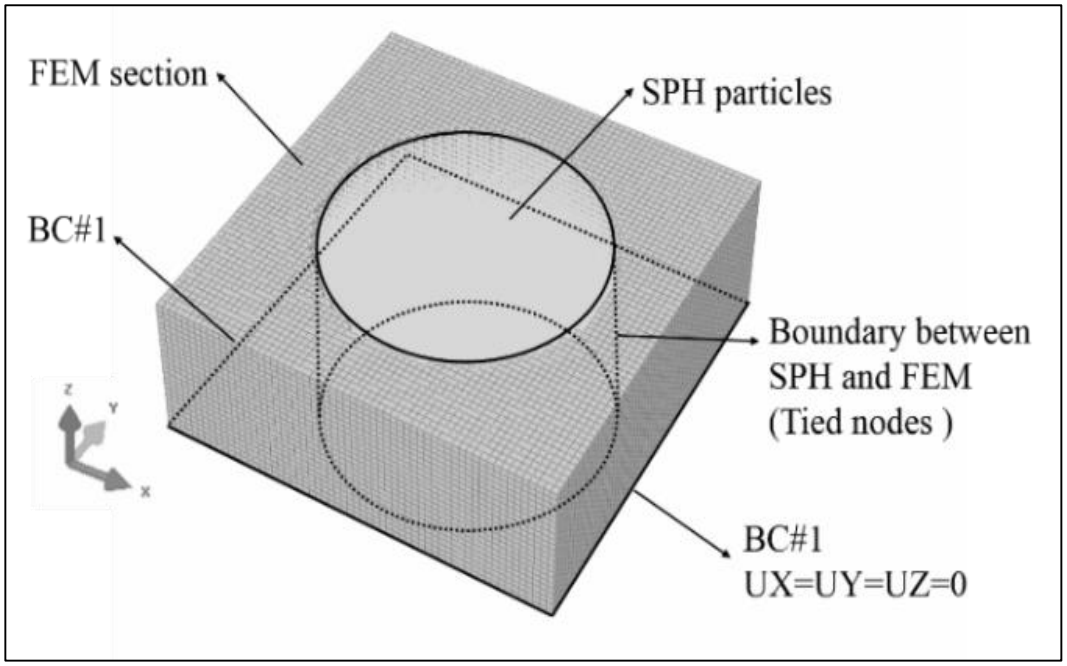

Figure 34: Hybrid model consisting of both SPH and FEM domains used for SPH simulation

For contact definition, “general contact” in ABAQUS was used. Specifically in FEM, the contact included two pairs: the entire surface of the drilling tool and all six faces of an element. The “element deletion” function was activated in FEM to allow an element to vanish when the element reaches its damage criteria. This permitted the tool to penetrate into the workpiece. The contact pair in the SPH models was the surface of the drilling tool and the particles. Note that an SPH particle was considered as an element but without any actual volume.

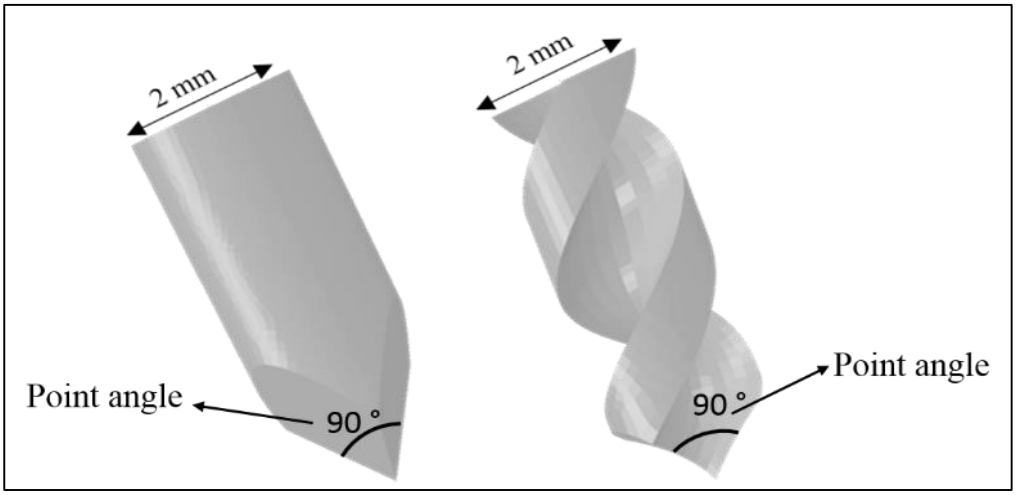

(a) (b)

Figure 35: Schematics of (a) the K-wire and (b) the twist drill

5.2 Numerical tests

This numerical study includes four cases consisting of K-wire and twist drill on two work-materials (one ductile and one brittle). The ductile material was chosen to be aluminum 2024-T351 and the brittle material is cortical bone.

Four case studies are identified as follows. Case 1 uses a twist drill to drill into the aluminum workpiece using FEM. Case 2 is the same to Case 1 but simulated by SPH. Case 3 uses K-wire to drill into the bone workpiece using FEM, and Case 4 uses SPH for the same setup as Case 3. In order to ensure a full contact between the cutting edges and the workpiece, two steps were defined in the simulation. In Step 1, the drill bit was advanced into the workpiece by a small distance to create initial contact. Step 2 initiated the drilling process. The feed rate in this step was set to be 7 mm/s for aluminum drilling along with a spindle speed of 800 RPM, which corresponded to 0.52 mm/rev (i.e., chip load). This feed rate ensured approximately 5 to 6 elements through the chip thickness.

The feed rate for the bone was 1 mm/s, which corresponded to 0.07 mm/rev. These parameters were randomly selected based on real practices. K-wire, by its nature, cannot be advanced as fast as a drill bit since there is no flute for separated chip to evacuate from the cutting zone. Forcing K-wire at a higher speed would cause the model to completely blow apart during drilling simulation. The friction coefficient between the drilling tool (stainless steel) and the specimen was set to be 0.2. This value was arbitrarily selected for the comparison purposes. Additionally, for both FEM and SPH models, mass scaling was employed to reduce the computational time. It was found no significant changes in force and torque responses of these models with mass scaling.

It is important to note that the purpose of this research is to compare SPH and FEM in the drilling of ductile and brittle materials instead of obtaining the absolute drilling forces. Thus, only a set of reasonable parameters is needed to perform the simulations.

5.3 Results

Drilling simulation results are presented in this section. The first comparison is between SPH and FEM in ductile drilling (Case 1 vs. Case 2). The second comparison is drilling of the brittle material with FEM and SPH methods (Case 3 vs. Case 4).

5.3.1 Aluminum drilling with twist drill

Figure 36 shows the simulation results at 0.029 s and 0.058 s for FEM and SPH model. Both models successfully drill into the work-material and create continuous chip as expected for the ductile material. However, it can be seen that the chip obtained by FEM has a different shape from that in SPH model. The curled chip of FEM is, in fact, closer to the reality of a plastically deformed work-material. SPH produces unrealistic

chip likely due to the numerical issues that occur on the free surfaces. SPH relies on the integration of the Kernel function across the particles in the simulation domain. Due to the lack of neighboring points at the free edges and surfaces (i.e., boundaries), SPH is unable to correctly calculate stress and strain on the free surfaces [33]. Therefore, since the cut chips contain a large free surface area, this free-surface effect could be magnified, which results in unrealistic chip formation. The higher stress distribution in the SPH chip is an evidence of this issue.

Figures 37 and 38 show the thrust force and torque, respectively, from SPH and FEM models. The first step that creates an initial contact is not shown in the chart. It can be observed that at the beginning of the simulation (about 0.04 s), both methods exhibit similar force and torque levels. Then, the two models begin to deviate from each other. The FEM produces a constant thrust force, and a nearly constant torque, in comparison with those of SPH. The thrust force and torque of FEM are closer to the theoretical phenomenon, provided a constant feed rate and spindle speed. The ramp-up force at the beginning of the data is when the cutting edges engage to the full chip load (i.e., feed per revolution). The oscillating profile is due to the resolution of the mesh size that causes some elements to vanish under extensive stress and excessive distortion. In contrast, SPH experiences a continuously increasing force and torque. This is due to the aforementioned numerical instability that happens on the free surfaces of the chip and creates higher stress (Figs. 29 and 31). The higher stress in the chip makes it stiffer than supposed to be, and thus requires higher forces to deform it and move along the flutes.

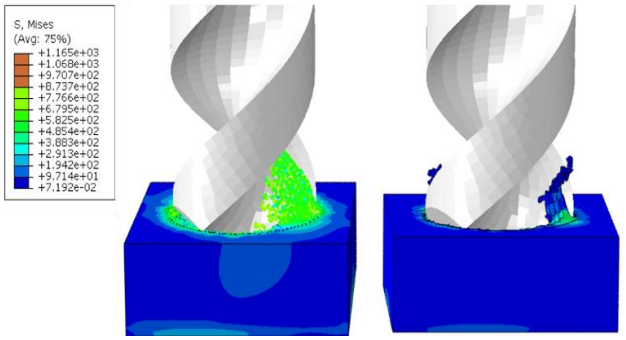

(a) 0.029 s (SPH) (b) 0.029 s (SPH)

(c) 0.058 s (SPH) (d) 0.058 s (FEM)

Figure 36: Simulation results of SPH vs. FEM for aluminum drilling with twist drill

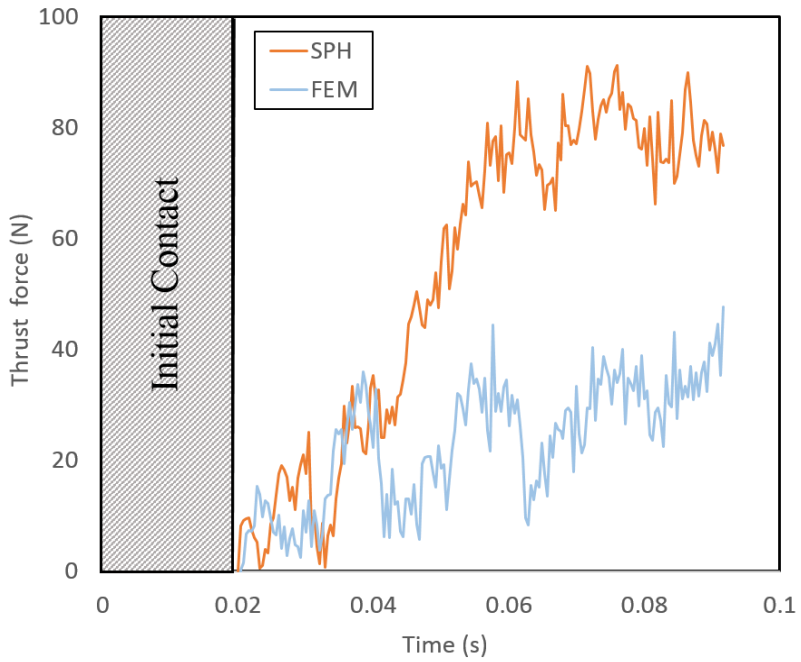

Figure 37: The FEM and SPH results of the thrust force for Al 2024-T351 drilling with twist drill

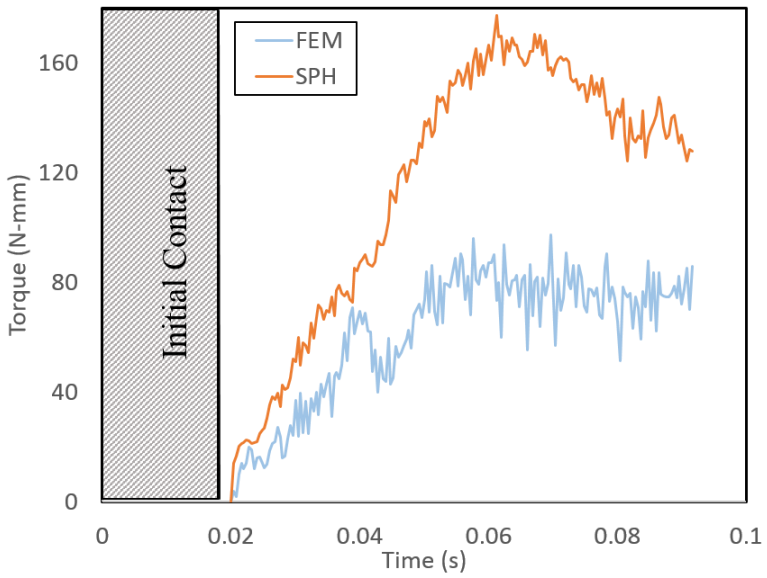

Figure 38: The FEM and SPH results of the drilling torque for Al 2024-T351 drilling with twist drill

5.3.2 Bone drilling with K-wire

Figure 39 shows the simulation results at 0.055 s and 0.068 s of both FEM and SPH models. In the SPH model, a large amount of small bone debris is separated from the model and accumulated on the surface of the workpiece. The zero-stress status of the accumulated particles on the surface is the evidence of a complete material damage (Figs. 39 (a) and (c)). Note the particles shown in the figure are for visualization in ABAQUS and they are not the actual volume of the debris. In contrast, FEM model does not produce any bone debris on the surface. This is because the element is disabled as soon as it reaches the damage criteria. As opposed to the SPH damage behavior that retains the particles and interactions with others, the failed elements in FEM are no longer involved in any calculations. As a result, the volume is gradually missing during the drilling process and the effect of debris cannot be incorporated. Bone debris accumulation is the primary cause

for K-wires being extremely hot (often over 100˚C) during deep hole bone drilling in orthopedic surgery [34].

For each case, the thrust force and torque were extracted and plotted in Figs. 40 and 41. Similarly, the data obtained from the first step is not shown here for the purpose of comparing material removal process only. The noisy data is likely due to the brittle nature and the distance between the particles (element size in FEM) relative to the chip load. In general, a smaller distance between the particles (finer FEM mesh) could result in smoother force profiles.

FEM has an oscillating result with a higher amplitude, which indicates an unstable drilling process. Unless the element size can be much smaller than the chip to form an entity, the element will vanish once it meets the defined damage criteria. The sudden loss of volume and contact results in the force drop. Therefore, the oscillating thrust force constantly decreases to zero during the simulation. However, this phenomenon is not reflected on the torque result due to the existence of friction between the tool and workpiece. As long as there is contact, the friction takes place in the tangential direction of the spinning tip, resulting in torque resistance.

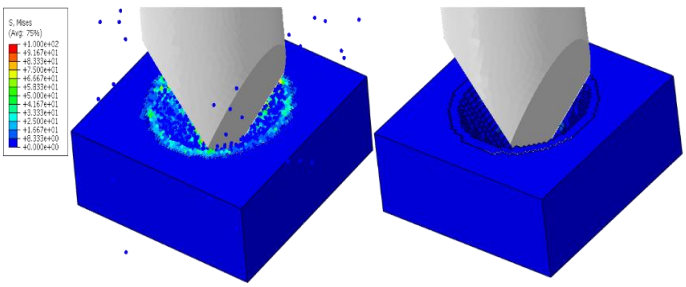

(a) 0.055 s (SPH) (b) 0.055 s (FEM)

Figure 39: Simulation results of SPH vs. FEM for bone with K-wire

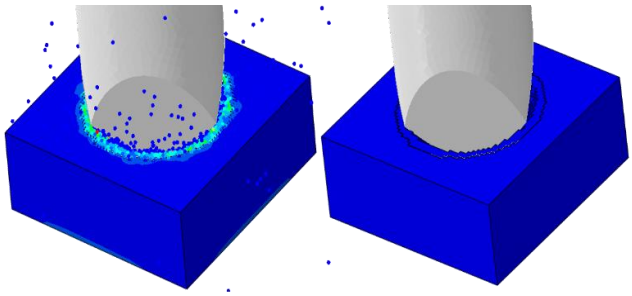

(c) 0.068 s (SPH) (d) 0.068 s (FEM)

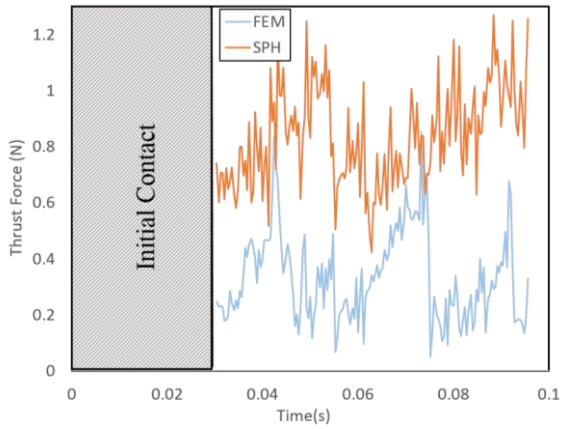

Figure 40: The FEM and SPH results of the thrust force for bone drilled with K-wire

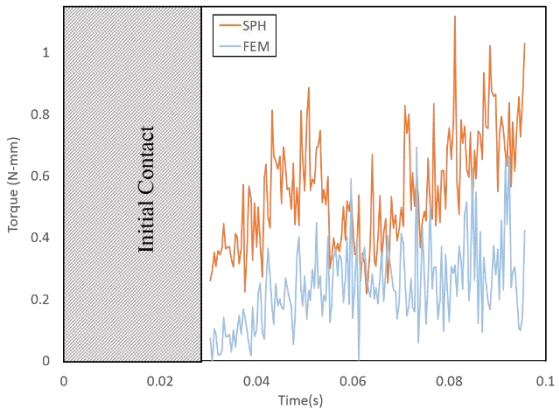

Figure 41: The FEM and SPH results of the drilling torque for bone drilled with K-wire

For the SPH model, it produces a slight increasing trend for both thrust force and torque. The results are closer to the reality [32]. Different from a regular drill bit, K-wire

does not have the flute to evacuate the debris and the accumulation can keep increasing the forces as the drilling proceeds.

CHAPTER VI

CONCLUSIONS AND FUTURE WORKS

6.1 Discussion

SPH has been demonstrated to be feasible to model drilling both ductile and brittle materials. In particular for brittle materials, SPH can handle small dusty chip formation and accumulation which are not simulated by the FEM. On the other hand, SPH demonstrated a stiffer behavior in ductile material drilling, which resulted in higher force and torque. Limitations and issues for SPH are attributed to three reasons. First, the numerical errors exist on the free surfaces due to the lack of neighboring points. Classical SPH approximation is not correctly calculated on the free surfaces[33]. As shown in Fig. 42 of a 1-D scenario, the kernel function is truncated at the free surfaces [35] and thus, the free surface shows an abnormal field value, which, in our case, transform to higher stress and strain. As a result, when a continuous chip is formed, more newly produced free surfaces can make the chip stiffer and stiffer. This issue may be solved by several free-surface treatment methods, such as renormalizing [33]. Commercial SPH solver, such as LS-DYNA and ABAQUS, both have this function to employ. However, since a drilling-produced chip involves a larger amount of particles on the free surfaces, compared to the interior particles, some other numerical issues are expected when using renormalization. Further investigation is needed.

Secondly, the particle distance of SPH (equivalent to the element size in FEM) plays an important role in drilling simulation. Convergence test is a common practice in

FEM, which ensures the element size not to significantly affect the simulation results. A finer mesh typically carries out more accurate results. Similarly for SPH, it is anticipated that a finer particle arrangement may mitigate the aforementioned free-surface issues and the oscillating force profile. However, significantly scaling down the particle distance of SPH will lose its advantages over FEM, such as capturing small dusty debris with a larger particle distance as shown in the results section (Fig. 39). Furthermore, SPH can significantly increase the computational time since it involves a tremendous neighboring particle searching. Trade-off between time and distance between particles is another limitation in SPH application.

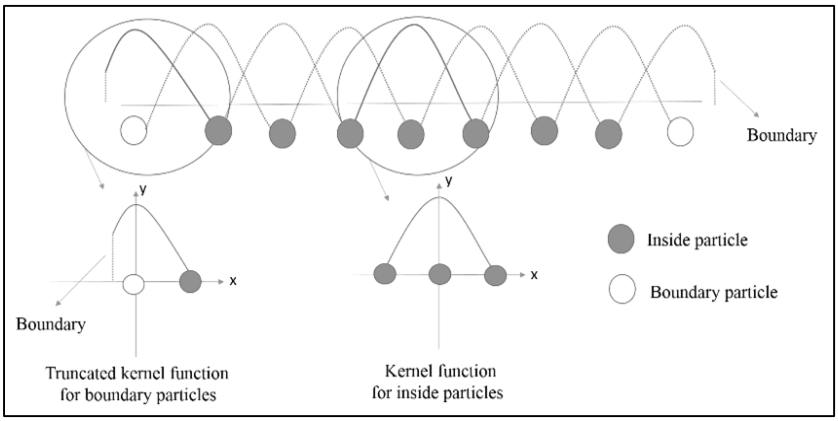

Figure 42: Truncated kernel function for free-surface particles vs. kernel function for interior particles (1-D model)

Third, damage criteria makes the SPH model unstable. It is required to manually tune damage settings including damage initiation and damage evolution to avoid "explosion" in the material removal process.

Lastly, it is important to note that this study is aimed at studying the feasibility of SPH in drilling as compared to conventional FEM models. The accuracy of the results has

not been quantitatively verified with experimental data. This means that it is uncertain if SPH can correctly incorporate the material parameters, such as friction coefficients and J-C models in the simulation.

6.2 Conclusions

This research presented the simulation of brittle and ductile material drilling with FEM and SPH model. It was found that FEM is more suitable for ductile material drilling since it can accurately produce continuous, cone-shape chips (in drilling simulations) and reasonable drilling force and torque profiles. On the contrary, to simulate brittle material drilling, SPH has superior performance due to the volume conservation where failed particles are not removed from the model. These particles continue to interact with cutting edge and workpiece to mimic the brittle debris interactions in dry or deep drilling.

6.3 Future works

SPH is still capable of simulating ductile material drilling. The discrepancy of the obtained drilling forces of two methods are the results of numerical errors on the free surfaces, particle distance effect and defining damage criteria. The future research will continue to investigate SPH in machining applications with the focuses on the issues discussed in this research and validation with experimental data.

REFERENCES

1. N. Schormair, K. Thuro, R. Plinninger, *The influence of anisotropy on hard rock drilling and cutting.* IAEG, Geological Society of London, UK, 2006.
2. K. Alam, M. Khan, V. V. Silberschmidt, *3D finite element modeling of drilling cortical bone: Temperature analysis.* Journal of Medical and Biological Engineering, 2014. 34(6), p. 618-623.
3. P. Krasauskas, S.K., R. Cesnavicius, D. Pacenga, *Experimental analysis and numerical simulation of the stainless AISI 304 steel friction drilling process.* Mechanika, 2014. 20(6), p. 590-595.
4. S. Usui, J. Wadell, T. Marusich, *Finite element modeling of carbon fiber composite orthogonal cutting and drilling.* 6th CIRP International Conference on High Performance Cutting (Hpc2014), 2014. 14, p. 211-216.
5. R.A. Williams, *A Study of the drilling process.* Journal of Engineering for Industry, 1974. 9(5), p. 343-345.
6. S. Yuan, C. Zhang, M. Amin, H. Fan, M. Liu, *Development of a cutting force prediction model based on brittle fracture for carbon fiber reinforced polymers for rotary ultrasonic drilling.* International Journal of Advanced Manufacturing Technology, 2015. 81(5), p. 1223-1231.
7. F. Ke, J. Ni, D. A. Stephenson, *Continuous chip formation in drilling.* International Journal of Machine Tools & Manufacture, 2005, p. 1652-1658.

8. W. A. Lughmani, K. Bouazza-Marouf, I. Ashcroft, *Drilling in cortical bone: a finite element model and experimental investigation.* Journal of the Mechanical Behavior of Biomedical Materials, 2014. 42, p. 32-42.

9. Y. Xi, M. Bermingham, G. Wang, M. Dargusch, *Finite element modeling of cutting force and chip formation during thermally assisted machining of Ti6Al4V alloy.* Journal of Manufacturing Science and Engineering, 2013. 135.

10. T. Thepsonthi, T. Ozel, *Experimental and finite element simulation based investigations on micro-millng Ti-6Al-4V titanium alloy: effects of cBN coating on tool wear.* Journal of Materials Processing Technology, 2012, p. 532-542.

11. G. List, G. Sutter, A. Bouthiche, *Cutting temperature prediction in high speed machining by numerical modelling of chip formation and its dependence with crater wear.* International Journal of Machine Tools & Manufacture, 2011, p. 1-9.

12. M. Elhachimi, S.Torbaty, P. Joyot, *Mechanical modelling of high speed drilling. 1:predicting torque and thrust.* International Journal of Machine Tools & Manufacture 1999, p. 553-568.

13. M. Calamaza, J.Limido, M. Nouaric, C. Espinosab, D. Couparda, M. Salaünb, F. Girota, R. Chieragattib, *Toward a better understanding of tool wear effect through a comparison between experiments and SPH numerical modeling of machining hard materials.* International Journal of Refractory Metals and Hard Materials, 2009. 27(3), p. 595-604.

14. Y. B. Guo, D.A. Dornfeld, *Finite element modeling of burr formation process in drilling 304 stainless steel.* Journal of Manufacturing Science and Engineering, 2000. 122(4).

15. T. D. Marusich, S.Usui, J. Ma, D. A. Stephenson, A. Shih, *Finite element modeling of drilling processes with solid and indexable tooling in metals and stack-ups.* 10th CIRP International Workshop on Modeling Operations, 2007, p. 51-57.

16. V. A. Phadnis, F.Makhdum, A. Roy, V. V. Silberschmidt, *Drilling in carbon/epoxy composites: Experimental investigations and finite element implementation.* Composites, 2012. 47, p. 41-51.

17. D. Che, J. Smith, K. F. Ehmann, *Finite element study of the cutting mechanics of the three dimensional rock turning process.* International Manufacturing Science and Engineering Conference 2015.

18. J. Limido, C. Espinosa, M. Salaun, J. L. Lacome, *SPH method applied to high speed cutting modelling.* International Journal of Mechanical Science, 2006, p. 898-908.

19. J. J. Monaghan, *Smoothed particle hydrodynamics.* IOPscience, 2005. 68, p. 1703–1759.

20. W. Benz, E. Asphaung, *Simulation of brittle solids using smooth particle hydrodynamics.* Computer physics communication, 1994. 87, p. 253-265.

21. P. W. Clearly, M. Prakash, J. Ha, *Novel applications of smoothed particle hydrodynamics (SPH) in metal cutting.* Journal of Materials Processing Technology, 2006. 177, p. 41-48.

22. T. Sakakibara, T. Tsuda, R. Ohtagaki, *SPH simulations of high velocity impacts on concrete plate.* 7th European LS-DYNA Conference, 2009.

23. T. Janakowiak, T. Lodygowsky, *Smoothed particle hydrodynamics versus finite element method for blast impact.* Bulletin of the Polish Academy of Sciences Technical Science, 2013. 61.

24. M. F. Villumsen, T.G. Fauerholdt, *Simulation of metal cutting using smooth particle hydrodynamics.* 7. LS-DYNA Anwenderforum, 2008.

25. Y. Altintas, *Manufacturing automation: metal cutting mechanics, machine tool vibrations, and CNC design.* 2012, Cambridge University Press.

26. T. Mabrouki, F.Giradin, M. Asad, J. F. Rigal, *Numerical and experimental study of dry cutting for an aeronautic aluminum alloy (A2024-T351).* International Journal of Machine Tools & Manufacture, 2009, p. 1187-1197.

27. W. Zhang, S. A. Tekalur, M. Baumann, L. R. McCabe, *The effect of damage accumulation the tensile strength and toughness of compact bovine bone.* Journal of Biomechanics, 2012, p. 964-972.

28. N. Ruttimann, S. Buhl, K. Wegenber, *Simulation of single grain cutting using SPH method.* Journal of Machine Engineering, 2010. 10.

29. S. S. Akarca, X. Song, W. J. Altenhof, A. T. Alpas, *Deformation behavior of aluminum during machining: modelling by Eulerian and smoothed-particle hydrodynamics methods.* Proceedings of the Institution of Mechanical Engineers, Part L: Journal of Materials Design and Applications, 2008. 222(3), p. 209-221.

30. M. Heinstein, D. Segalman, *Simulation of orthogonal cutting with smooth particle hydrodynamics.* Sandia National Laboratories, Livermore, California, 1997.

31. R. De Borst, M. A. Crisfield, J. J. C. Remmers, C. V. Verhoosel, *Nonlinear finite element analysis of solids and structures*. 2012, John Wiley & Sons.

32. B. L. Tai, F. Nonoyama., Y. Wang, A. J. Shih, *Enhancement of Kirschner wire for bone drilling.* International Manufacturing Science and Engineering Conference, 2014.

33. C. Espinosa, J. Lacome, J. Limido, M. Salaun, *Modeling high speed machining with the SPH method.* 10th International LS-DYNA Users Conference, 2008.

34. L. S. Matthews, C. Hirsch, *Temperatures measured in human cortical bone when drilling.* Journal of Bone and Joint Surgery, 1972. 54, p. 297-308.

35. M. Liu, G. Liu, *Smoothed particle hydrodynamics (SPH): an overview and recent developments.* Archives of Computational Methods in Engineering, 2010. 17(1), p. 25-76.